摘 要

我們以瞬間正則模的方法計算水在偶極感應下的拉曼光譜，在此方法，每個瞬間正則模對polarizability anisotropy INM spectrum 的貢獻權重不一。此論文中，計算了每個模的權重因子。我們也藉由比較分子動力模擬方法而得的拉曼光譜來討論此方法所得的結果。

另一方面，也探究了水的低頻譜的緣由。低頻譜的微觀來由還未有一致的論點。此論文使用Voronoi多面體分析來研究局部結構對水的拉曼光譜的影響。雖然結果並不夠清楚來辨識局部結構對水拉曼光譜的影響，但新的方法(Voronoi多面體分析應用於水的拉曼光譜)已被探究。

Abstract

We have calculated the Raman spectrum of liquid water in dipole-induced-dipole interaction in terms of instantaneous normal mode method. In this method, polarizability anisotropy INM spectrum is calculated with each INM weighted differently, where "INM"is abbreviated from "instantaneous normal mode". In this thesis, the weighting factor of each INM is calculated. We also discuss the results of Raman spectrum in INM method by comparing with those obtained by the MD simulation.

On the other hand, the origin of the low-frequency spectrum of water is also studied. Designations for the origin of the low-frequency spectrum from microscopic point of view are still not determined. In this thesis, the Voronoi polyhedral analyses are used for investigating the effect of local structure on Raman spectrum of liquid water. Although the results are not clear enough to identify the effect of local structures in Raman spectrum of liquid water, new approach (VP analyses on Raman spectrum) has been studied.

誌 謝

一本論文的誕生，意味著人生旅途的一個段落。回首碩士班的這兩年旅程，所受到的恩典，細細回想，足令人動容。

感謝昆憲學長，從碩一開始學習電腦軟硬體、程式的教學、模擬方法等等，在研究上一路的提供很多的協助與細心地教導。

感謝邦杰學長，在計算上的輔助、並熱切與耐心地讓我諮詢大大小小的問題。

感謝平翰兄，一路相伴在左，在我研究上有困頓時，可以有人請教，適時得到協助，得以繼續進行。

最後尤其感謝天鳴老師，除了提供研究環境資源、循序漸進式的帶領，讓我體會按部就班，從做中學等學習與處事方法，也很感謝老師對學生的關心與教誨。

一路走來，能夠順遂，全歸計算模擬實驗室的幫助與提攜，當然，還有其他許多人曾經做過的努力，使我可以站在巨人的肩膀上做研究。

除了在研究上的精進，生活上，幸運有知心好友們的傾聽與指點、交大豐富的人事物，讓我的心胸、想法開拓不少。

能進入交大的環境，從事一點科學研究的機會，還須感謝一大群人，尤其是父母、家人，及師長們的支持與鼓勵。

最後，在未來的旅程上，帶著這些曾受過恩賜，向前邁進！

Contents

List of Figures

List of Tables

Chapter 1

Introduction

Since 1930s, the low-frequency spectrum of liquid water has been detected by several experimental techniques[1][2]. In the spectrum, there are two bands, 60 cm^{-1} and 180 cm^{-1}. Interpretation of the origins of these band from microscopic point of view are in dispute. Designation of the high frequency, 180 cm^{-1}, is H bond stretching or O...O stretching, and they are similar in physics. As to the lower frequency, 60 cm^{-1} band, there are many designations for it. Here are a series of examples. Walrafen and co-workers[3] assigned this band to the bending of a triplet cluster, which is one molecule and two H-bonded neighbors(Fig.2.1). The bending motion is perpendicular to a H-bond. Also, the two bands under the interpretation of triplet cluster are considered as arising from the restricted translations. However, Padro and Marti[1] give a different interpretation that this band should not be related to hydrogen bond, because an analogous frequency band in density of states obtained by velocity autocorrelation function is also found in nonhydrogen liquids. It should be translations frustrated by cage effect. De Santis et al.[4] later commented that both of two low-frequency bands can be obtained in density of states of melting and supercooled liquids of argon, but the cage form by four H-bonds enhance the intensity of density of states when comparing with it. Therefore, both of the bands are due to the H-bond formation.

The motivation of this research is to study the origin of the low-frequency spectrum of water. The Voronoi polyhedral analyses has been used to analysis the local structures of liquid water. This analysis was used to study the roles of local structures in the relaxation of orientational dynamics via MD simulation[5], and this analysis indicates that the Voronoi polyhedra of water molecules are highly deviated from sphericity, and the local structures are basically tetrahedral. Recently, this analysis was applied to the density of states

for liquid water[2][6]. The result on the translational density of states[2] indicates that the 60 cm^{-1} band is O...O...O bending mode. In this research, the Voronoi polyhedral analyses are used for investigating the effect of local structure on Raman spectrum of liquid water.

There are two ways to calculate Raman spectrum. One is caculated by MD simulation. The other is called the INM method. In MD simulation, depolarized Raman spectrum is evaluated via time autocorrelation function of anisotropic part of collective polarizability tensor. In INM method, because collective polarizability of a system is a function of molecular coordinates, it can be expressed by normal modes. INM analysis is used to evaluate depolarized Raman spectrum for short time approximation. But INM method only need initial equilibrium configurations and some eigen-analysis which does not involve time. By the INM method, the spectrum is obtained without the dynamics[7].

In this thesis, theoretical approaches including basic INM theory and Voronoi polyhedral analysis are described in the following chapter. In chapter 3, Raman spectrum $R(\omega)$ by MD simulation and INM calculational method, and Vorronoi polyhedra analysis applying to Raman spectrum are introduced. Chapter 4 shows the results of Raman spectrum and Voronoi analyses. In the last chapter, we summarize our works and give conclusions of this thesis.

Chapter 2

Theoretical Methods

2.1 Molecular dynamics (MD) simulation

In this introduction, equilibrium configurations of liquid water generated by the method of MD simulation are analyzed by the INM approach. The model of water we adopted is SPC/E, a three-site rigid model. In the SPC/E model, the potential energy is the sum of the Coulomb interactions and the LJ interactions[8].

$$V = \frac{1}{2} \sum_{i,j(\neq i)} \left[\sum_{\alpha,\beta} \frac{q_{i\alpha} q_{j\beta}}{r_{i\alpha,j\beta}} + 4\varepsilon \left((\frac{\sigma}{r_{iO,jO}})^{12} - (\frac{\sigma}{r_{iO,jO}})^{6}) \right) \right]. \qquad (2.1)$$

$r_{i\alpha,j\beta}$ is the distance between α site of molecule i and β site of molecule j. The parameters of SPC/E model are given in Table 1, and the model of water molecule is shown in Fig. 2.2. Following the previous works [8], we collected the configurations every 400fs, so that the the configurations should be less correlated to avoid the statistic error in ensemble average. In our simulation, the temperature and density of water are 300K and 1g/ cm^3, respectively. The number of molecules in simulation is 256, and the periodic boundary conditions are used.

2.2 Basic instantaneous normal mode (INM) theory for rigid model of liquid water

2.2.1 Introduction of INM theory

In classical mechanics, once an initial state is given, the dynamics of this system in later time is determined. Here, the initial state is generated by MD simulation. That is, we can solve the eq. of motion by simulation, and

obtain the solutions for the evolution of the positions and velocities of the water molecules in the system. The molecules in the liquid system interact with each other, and their dynamics are coupled together. However, we can always find a set of normal coordinates, which describe the motions with specific frequencies in virtue of the INM approximation[10].

The following is the INM formalism[8][11][12].

2.2.2 The INM Hamiltonian

The dynamic properties of a system is determined by its Hamiltonian[13]. The Hamiltonian can be represented by different kinds of coordinates.

- General coordinates

  The Hamiltonian is the sum of kinetic energy of all molecules in the system and the potential energy of the system. The kinetic energy is composed of the translational and rotational parts of each rigid molecule.

$$H = \sum_j \left(\frac{1}{2} m \dot{\mathbf{r}}_j^2 + \frac{1}{2} \sum_\mu I_{j\mu} \omega_{j\mu}^2 \right) + V(\mathbf{R}) \tag{2.2}$$

  where m denotes the mass of a water molecule and $\mathbf{r}_j = \{X_j, Y_j, Z_j\}$ denotes the center-of-mass position of molecule j. $I_{j\mu}$ is the momentum of inertial along principle axis $\mu = \{x, y, z\}$ for molecule j and $\omega_{j\mu}$ is the angular velocity along molecular axis μ, which rotates with the molecule observed in the lab. frame, as represented in Fig.2.4. The orientations of molecular axes are determined by a set of Euler angles $\mathbf{\Omega} = \{\phi, \theta, \psi\}$ observed in the lab. frame[14][15]

$$\begin{pmatrix} \omega_{jx} \\ \omega_{jy} \\ \omega_{jz} \end{pmatrix} = \begin{pmatrix} \sin\theta_j \sin\psi_j & \cos\psi_j & 0 \\ \sin\theta_j \cos\psi_j & -\sin\psi_j & 0 \\ \cos\theta_j & 0 & 1 \end{pmatrix} \begin{pmatrix} \dot{\phi}_j \\ \dot{\theta}_j \\ \dot{\psi}_j \end{pmatrix}. \tag{2.3}$$

  V($\mathbf{R}$) given in eq.2.1 are a function of $\mathbf{R}$= $\{\mathbf{r}_j, \mathbf{\Omega}_j\}$, for j=1,2,...,N, which is the general coordinates of a configuration.

- Mass-weighted generalized coordinates

  We define the 6N-dimensional mass-weighted coordinates

$$\boldsymbol{Z} = \{\boldsymbol{z}_j\},\ j = 1, \ldots, N, \tag{2.4}$$

and the components of $\boldsymbol{z}_j$,

$$\begin{aligned}\boldsymbol{z_j} &= \{z_{j\mu}\},\ \mu = 1, \ldots, 6 \\ &= \{\sqrt{m}x_j, \sqrt{m}y_j, \sqrt{m}z_j, \sqrt{I_x}\zeta_{jx}, \sqrt{I_y}\zeta_{jy}, \sqrt{I_z}\zeta_{jz}\},\end{aligned} \tag{2.5}$$

$\boldsymbol{\zeta}_j$ is the orientation of molecule j and is expressed in the body frame for the instantaneous configuration $\mathbf{R}_0 = \{\mathbf{r}_j^0, \boldsymbol{\Omega}_j^0\}$, where $\boldsymbol{\Omega}_j^0 = \{\phi_j^0, \theta_j^0, \psi_j^0\}$

$$\begin{pmatrix}\zeta_{jx}\\ \zeta_{jy}\\ \zeta_{jz}\end{pmatrix} = \begin{pmatrix}\sin\theta_j^0 \sin\psi_j^0 & \cos\psi_j^0 & 0\\ \sin\theta_j^0 \cos\psi_j^0 & -\sin\psi_j^0 & 0\\ \cos\theta_j^0 & 0 & 1\end{pmatrix}\begin{pmatrix}\phi_j\\ \theta_j\\ \psi_j\end{pmatrix}, \tag{2.6}$$

where $\boldsymbol{\zeta}_j$ and $\boldsymbol{\Omega}_j$ are functions of t*.

In the mass-weighted coordinates, the Hamiltonian can be expressed as

$$H = \frac{1}{2}\dot{\mathbf{Z}}\dot{\mathbf{Z}} + V(\mathbf{Z}). \tag{2.7}$$

In the INM approximation, we expand $V(\boldsymbol{Z})$ in a Taylor series up to the second order with respect to the displacement at time t from t=0, and

$$H = \frac{1}{2}\dot{\mathbf{Z}}\dot{\mathbf{Z}} + V(\mathbf{R}_0) - \mathbf{F}(\mathbf{R}_0)(\mathbf{Z}_t - \mathbf{Z}_0) + \frac{1}{2}(\mathbf{Z}_t - \mathbf{Z}_0)\mathbf{D}(\mathbf{R}_0)(\mathbf{Z}_t - \mathbf{Z}_0), \tag{2.8}$$

where $\mathbf{F}(\mathbf{R}_0)$ is a 6N-dimensional force vector whose elements are

$$F_{j\mu}(\mathbf{R}_0) = -\left.\frac{\partial V(\mathbf{R})}{\partial z_{j\mu}}\right|_{\mathbf{R}_0} \tag{2.9}$$

and

$$D_{(j\mu)(k\nu)}(\mathbf{R}_0) = \left.\frac{\partial V(\mathbf{R})}{\partial z_{j\mu}\partial z_{k\nu}}\right|_{\mathbf{R}_0} \tag{2.10}$$

- Instantaneous normal coordinates

  Let $\mathbf{U}(\mathbf{R}_0)$ be 6N×6N orthogonal matrix, which comprise 6N eigenvectors of Hessian matrix $\mathbf{D}(\mathbf{R}_0)$. As well known, $\mathbf{U}(\mathbf{R}_0)$ is the matrix which transforms Hessian matrix in the mass-weighted coordinates$\{z_{j\mu}\}$ into that in normal coordinates $\{q_\alpha\},\ \alpha = 1, 2, \ldots, 6\text{N}$.

  $\mathbf{D}(\mathbf{R}_0)$ in the normal coordinates is diagonalized, and expressed as $\mathbf{A}$

$$\mathbf{A} = \mathbf{U}^T\mathbf{D}\mathbf{U}, \tag{2.11}$$

*$\boldsymbol{\zeta}$ is the same physical observation with Euler angle $\boldsymbol{\Omega}_j$, but is observed in the body frame whose axes are assumed to be fixed instantaneously.

with elements to be the eigenvalues of $\mathbf{D}(\mathbf{R}_0)$

$$\omega_\alpha^2 = \sum_{j\mu,k\nu} U_{\alpha,j\mu} D_{j\mu,k\nu} U_{k\mu,\alpha} \tag{2.12}$$

The transformed forces are given as

$$f_\alpha(\mathbf{R}_0) = \sum_{j\mu} U_{\alpha,j\mu}(\mathbf{R}_0) F_{j\mu}(\mathbf{R}_0) \tag{2.13}$$

and the instantaneous normal coordinates are

$$q_\alpha(t, \mathbf{R}_0) = \sum_{j\mu} U_{\alpha,j\mu}(\mathbf{R}_0)[z_{j\mu}(t) - z_{j\mu}(0)]. \tag{2.14}$$

The Hamiltonian in eq.(2.8), can be rewritten by as

$$H = V(\mathbf{R}_0) + \sum_{\alpha=1}^{6N} \left(\frac{1}{2}\dot{q}_\alpha^2 + \frac{1}{2}\omega_\alpha^2 q_\alpha^2 - f_\alpha q_\alpha \right). \tag{2.15}$$

If we defined the shifted normal coordiates

$$x_\alpha \equiv q_\alpha - \frac{f_\alpha}{w_\alpha^2} \tag{2.16}$$

the Hamiltonian is written as the form

$$H = V(\mathbf{R}_0) + \sum_{\alpha=1}^{6N} \left(\frac{1}{2}\dot{x}_\alpha^2 + \frac{1}{2}\omega_\alpha^2 x_\alpha^2 - \frac{f_\alpha}{2\omega_\alpha^2} \right). \tag{2.17}$$

The physical picture of the INM approximation is discribed in Fig. 2.5

2.2.3 The INM dynamics and density of states

The Harmiltonian in eq.(2.17) is a set of 6N harmonic oscillators, and its dynamic solutions are

$$x_\alpha(t) = x_\alpha(0)\cos\omega_\alpha t + \frac{\dot{x}(0)}{\omega_\alpha}\sin\omega_\alpha t \tag{2.18}$$

$$v_\alpha(t) \equiv \dot{x}_\alpha(t) = \dot{x}_\alpha(0)\cos\omega_\alpha t + x_\alpha(0)\omega_\alpha \sin\omega_\alpha t \tag{2.19}$$

The velocity autocorrelation function of any normal mode is

$$\langle v_\alpha(0) v_\alpha(t) \rangle = k_B T \cos(w_\alpha t), \tag{2.20}$$

because velocities and positions of molecules are independent with one another, $< \dot{x}_\alpha(0) x_\beta(0) >= 0$ and the velocity autocorrelation function of the initial conditions give $< v_\alpha(0) v_\beta(0) >= k_B \mathrm{T} \delta_{\alpha\beta}$ from the equipartition theorem.

Averaged over a liquid configuration which has 6N degrees of freedom, the velocity autocorrelation function can be expressed in terms of frequency spectrum.

$$\frac{1}{6N}\sum_{\alpha=1}^{6N} < v_\alpha(0)v_\alpha(t) >= k_B T \int dw D(w)\cos(wt), \tag{2.21}$$

where

$$D(w) =< \frac{1}{6N}\sum_{\alpha=1}^{6N}\delta(w - w_\alpha) >, \tag{2.22}$$

is the normalized density of states. $\int D(\omega)dw = 1$. Because the number of modes of a condensed system is large and the mode frequencies of a system are dense, the density of states are usually represent by the average number of modes within a frequency window, so that the normalized density of states depicts the probability distribution of normal modes.

2.3 Voronoi polyhedral analyses for local structures

The Voronoi cell of a particle in a liquid system is the smallest polyhedron formed by equi-partitional planes between any two particles, so that there is only one particle in the Voronoi cell. Any point inside the Voronoi cell of a particle is closer to that particle than any other ones. Voronoi cell is therefore a generalization of the Wigner-Seitz unit cell of a crystal. In this thesis, the Voronoi polyhedra of the O atoms are classified into four groups according to two kinds of dimensionless parameters, asphericity η and the scaled volume $\tilde{V}$, which are defined as[2] [6]

$$\eta = \frac{A^3}{36\pi V^2} \tag{2.23}$$

and

$$\tilde{V} = \frac{V}{V_{avg}}, \tag{2.24}$$

where V and A are the volume and surface of a Voronoi polyhedron, respectively. V_{avg} is the averaged volume per molecule in the system. The ranges of η or $\tilde{V}$ for the four groups defined in the thesis are given in Table 3.

In formalism, selection operator $\Theta_i(L)$ is introduced to specify Voronoi groups.

$$\Theta_i(L) = \begin{cases} 1 & \text{if molecule i belongs to Voronoi group L} \\ 0 & \text{otherwise} \end{cases}$$

Summation of the four selection operators equals to identity operator.

$$\sum_{L=I}^{IV} \Theta_i(L) = 1 \tag{2.25}$$

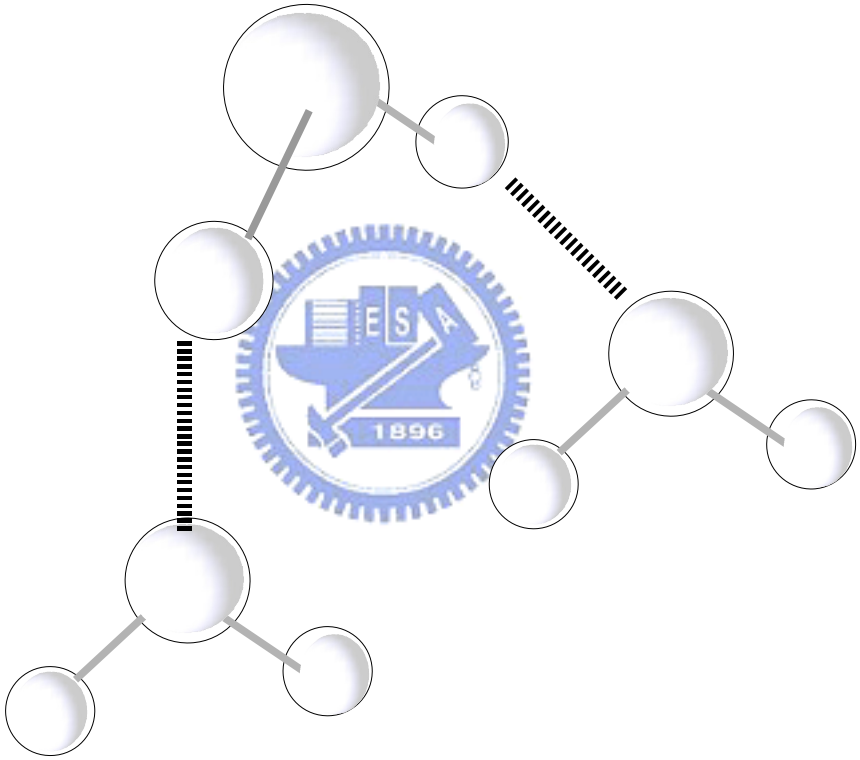

Figure 2.1: Triplet cluster of water. The dashed lines represent hydrogen bonds.

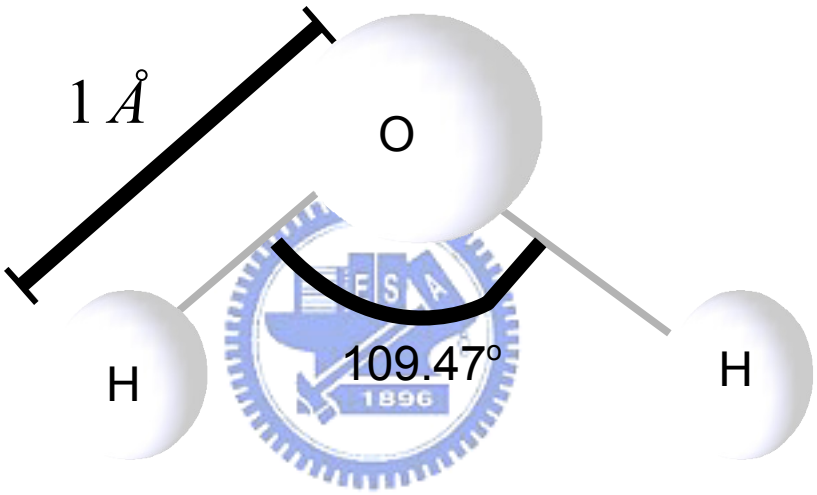

Figure 2.2: Water molecule in the SPC/E model.

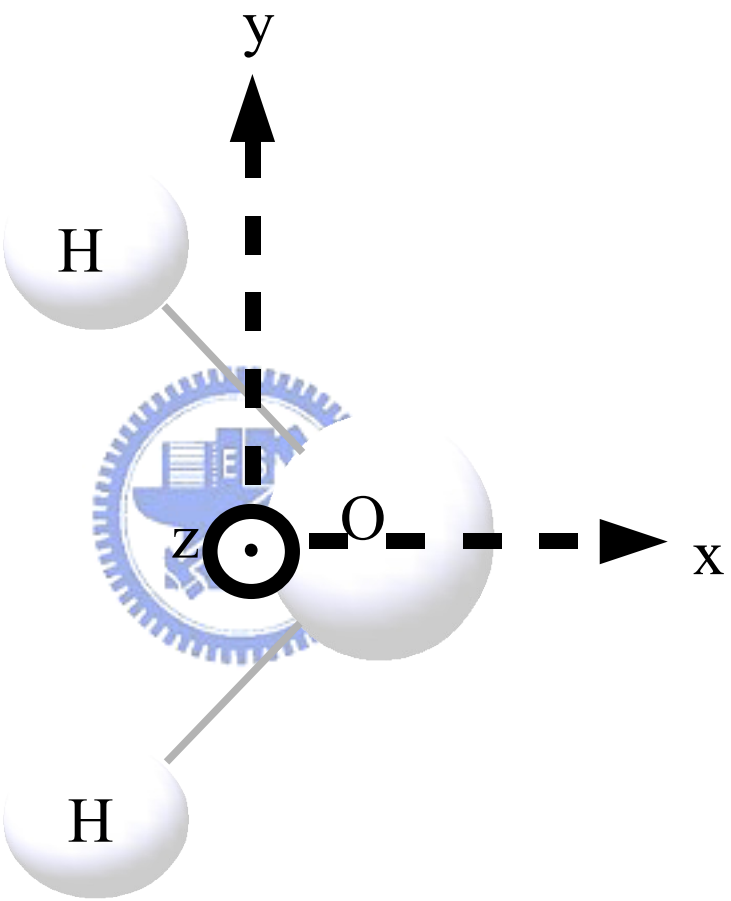

Figure 2.3: Water molecular axes

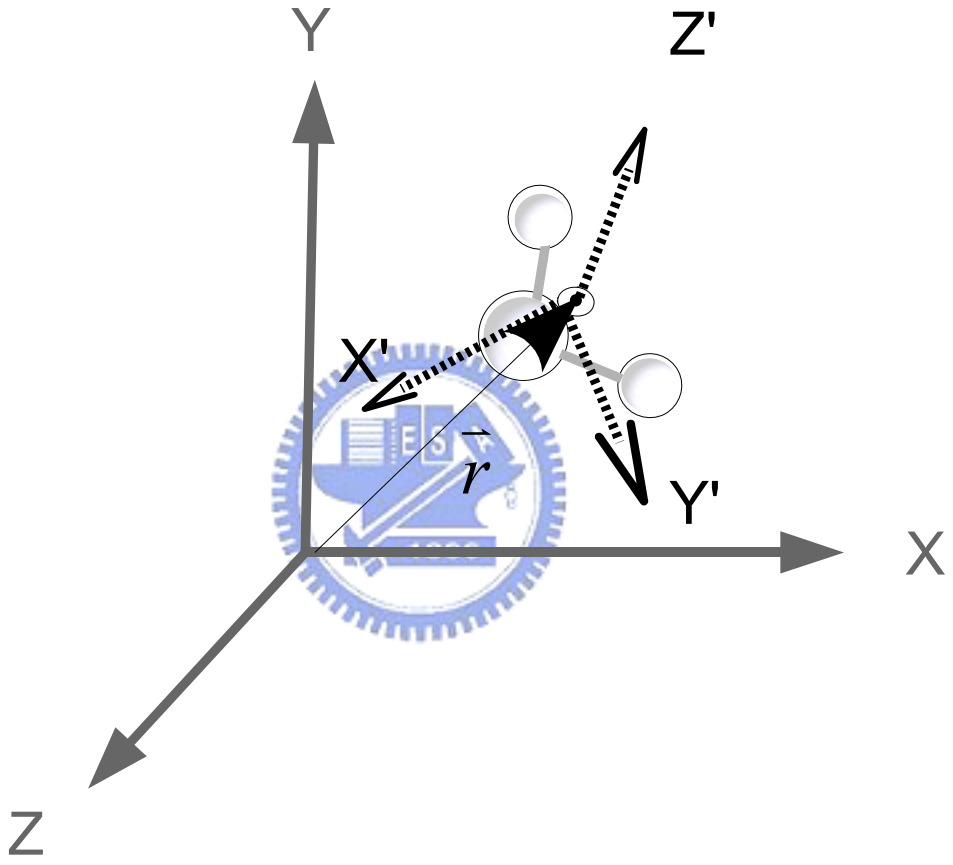

Figure 2.4: The coordinate axes(X, Y, Z) in the lab. frame and the molecular axes(X', Y', Z') in the body frame. $\vec{r}$ is the center of mass of the molecule.

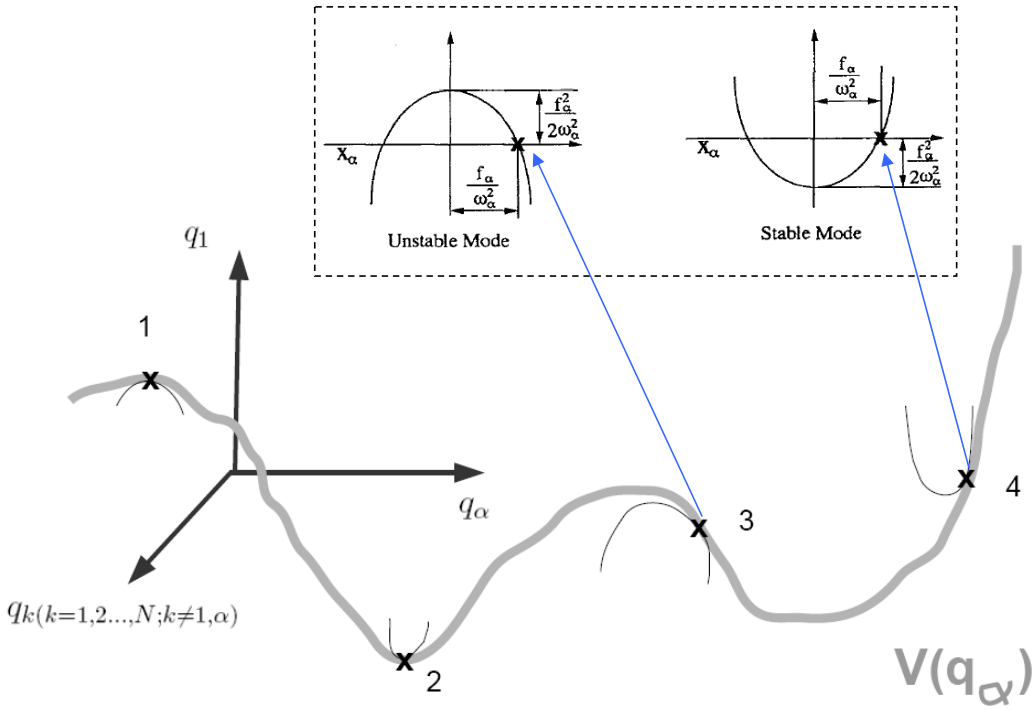

Figure 2.5: The INM approach. The point X at the potential energy hypersurface represents the potential of specific configuration. Consider α-direction, potential is depicted by a parabola as using INM approach. Configuration 1 and 2 are at the extreme of the hypersurface and also in the equilibrium of the INM approach harmonic oscillation; configuration 3 and 4 do not. The shift quantity $\frac{f_\alpha}{\omega_\alpha^2}$ from an extreme of INM approach parabola is the displacement from the equilibrium of INM approach harmonic oscillation at t=0. Two figures in the insets are referred from Ref.[11]

Chapter 3

Depolarized Raman Spectrum

3.1 MD method

The depolarized Raman spectrum $R(\omega)$ is expressed by[16]

$$R(\omega) = (1 - e^{-\hbar\omega/k_BT}) \int_0^\infty dt \, \sin(\omega t)[-\frac{\partial \Psi(t)}{\partial t}], \tag{3.1}$$

with $\Psi(t)$ the time correlation function of the off-diagonal component of the collective polarizability tensor, which is defined as

$$\Psi(t) = \frac{15}{N\gamma^2}\langle \Pi_{xz}(0)\Pi_{xz}(t)\rangle, \tag{3.2}$$

where $\gamma = \frac{1}{2}[(\alpha^0_{11}-\alpha^0_{22})^2+(\alpha^0_{22}-\alpha^0_{33})^2+(\alpha^0_{11}-\alpha^0_{33})^2]$ is polarizability anisotropy and α^0_{mm} the principle polarizability components.

Nuclear response function is defined as

$$R_{nuclei}(t) = -\frac{1}{k_BT}\frac{\partial \Psi(t)}{\partial t}, \tag{3.3}$$

which can be detected by OKE experiments. The OKE experimental signal in the time domain is sensitive to the ultrafast intermolecular dynamics that affects the electric polarization of the liquid molecular system.[17]

The nuclear response function represented in the frequency domain is called OKE spectrum $\chi(\omega)$,

$$\mathrm{Im}[\chi(\omega)] = \int_0^\infty \sin(\omega t) R_{nuclei}(t) dt. \tag{3.4}$$

Depolarized Raman spectrum is related to the OKE spectrum through the following formula

$$R(\omega) = (1 - e^{-\hbar\omega/k_BT})\mathrm{Im}[\chi(\omega)], \tag{3.5}$$

where $(1 - e^{-\hbar\omega/k_BT})$ is the quantum correction factor.

3.2 INM theory of polarizability anisotropy dynamics

Polarizability anisotropy velocity time correlation is defined as the second derivative of $\Psi(t)$ with respect to t

$$G_{xz}(t) = -\ddot{\Psi}_{xz}(t). \tag{3.6}$$

According to the definition of $\Psi(t)$ in eq.(3.2) and the property of second derivative of time correlation function with respect to t *[18],

$$G_{xz}(t) = -\frac{15}{N\gamma^2}\langle\Pi_{xz}(0)\ddot{\Pi}_{xz}(t)\rangle = \frac{15}{N\gamma^2}\langle\dot{\Pi}_{xz}(0)\dot{\Pi}_{xz}(t)\rangle. \tag{3.7}$$

$G_{xz}(t)$ is time correlation function of the first derivative of off-diagonal element of polarizability, and is named as the polarizability anisotropy velocity time correlation function.

The following is the INM theory for expressing $G_{xz}(t)$ in terms of normal coordinates q_α[19]. The collective polarizability depends on the coordinates of molecules, and we expand off-diagonal element of the collective polarizability in terms of normal modes first.

$$\begin{aligned}&\Pi_{xz}(t) = \Pi_{xz}(q_\alpha(t)) \\ =&\Pi_{xz}(q_\alpha(0)) + \sum_\alpha \left(\frac{\partial\Pi_{xz}}{\partial q_\alpha}\right)_{t=0} q_\alpha(t) + \sum_\alpha\sum_\beta \left(\frac{\partial\Pi_{xz}}{\partial\, q_\alpha\partial q_\beta}\right)_{t=0} q_\alpha q_\beta + \cdots .\end{aligned} \tag{3.8}$$

Then, by using the linear approximation (the INM approximation for short time), the quadratic and higher-order terms can be neglected. This approximation gives

$$\dot{\Pi}_{xz}(t) \cong \sum_\alpha \left(\frac{\partial\Pi_{xz}}{\partial q_\alpha}\right)_{t=0} \dot{q}_\alpha(t). \tag{3.9}$$

Finally, substitute the approximated $\dot{\Pi}_{xz}(t)$ in eq.(3.9) into eq.(3.7)

$$G_{xz}(t) \cong \frac{15}{N\gamma^2}\langle\sum_\alpha \left(\frac{\partial\Pi_{xz}}{\partial q_\alpha}\right)_{t=0} \dot{q}_\alpha(0) \sum_\beta \left(\frac{\partial\Pi_{xz}}{\partial q_\beta}\right)_{t=0} \dot{q}_\beta(t)\rangle. \tag{3.10}$$

Since the velocity($\dot{q}$) and position(q) of each molecule are independent, the velocity($\dot{q}$) can be seperated apart from position(q). Also different degrees of freedom are independent, the correlation function of cross terms of different degrees vanish. The velocity autocorrelation of INM, eq.(2.20), is used, hence

$$G_{xz}(t) \cong k_B T\frac{15}{N\gamma^2}\sum_\alpha \langle\left(\frac{\partial\Pi_{xz}}{\partial q_\alpha}\right)^2\rangle_{t=0} \cos(\omega_\alpha t) \tag{3.11}$$

* $\frac{d^2}{dt^2}\langle B(t)A\rangle = -\langle\dot{B}(t)\dot{A}(t)\rangle$

Through above derivation, we replace the summation with integral.

$$G_{xz}(t) = k_B T \int \rho_{pol}(\omega) \cos(\omega t) d\omega, \tag{3.12}$$

where

$$\rho_{pol}(\omega) = \frac{15}{N\gamma^2} \sum_{\alpha} \langle (\frac{\partial \Pi_{xz}}{\partial q_\alpha})^2 \delta(\omega - \omega_\alpha) \rangle \tag{3.13}$$

is polarizability anisotropy INM spectrum. The normalized spectrum is

$$D_{pol}(\omega) = \frac{\rho_{pol}(\omega)}{\int \rho_{pol}(\omega) d\omega}. \tag{3.14}$$

Compared with the density of states (eq.(2.22)) of liquid water which has been reported[8], the polarizability anisotropy INM spectrum is similar as the density of states (DOS), but each mode is weighted by a factor $(\frac{\partial \Pi_{xz}}{\partial q_\alpha})^2$. The polarizability anisotropy velocity time correlation G_{xz} and polarizability anisotropy INM spectrum ρ_{pol} (eq.(3.12) and eq.(3.13)) are analogous to the velocity autocorrelation function and the density of states (eq.(2.21) and (2.22)), respectively. One is in time domain, and the other is in frequency domain.The relation between them is a Fourier transformation[†].

3.3 The correlation between polarizability anisotropy INM spectrum $\rho_{pol}(\omega)$ and depolarized Raman spectrum $\mathbf{R}(\omega)$

From eq.(3.1) and eq.(3.3),

$$R(\omega) = k_B T [1 - e^{-\hbar\omega / k_B T}] \int_0^\infty dt \, \sin(\omega t) R_{nuclei}(t). \tag{3.15}$$

R_{nuclei}(t) is proportional to $\frac{\partial \Psi(t)}{\partial t}$ (eq.(3.3)), and by the definition of G_{xz}(t)(eq.(3.6)), $\frac{\partial \Psi(t)}{\partial t}$ is proportional to integral of G_{xz}(t)

$$R_{nuclei}(t) = \frac{1}{k_B T} \int_0^t G_{xz}(\tau) d\tau. \tag{3.16}$$

By means of the substitution of eq.(3.12) and the integral with respect to τ from 0 to t,

$$R_{nuclei}(t) = \int \rho_{pol}(\omega) \frac{\sin \omega t}{\omega} d\omega. \tag{3.17}$$

[†]Because autocorrelation is even function, Fourier cosine transformation of spectrum is used, and we used to plot positive regime of spectrum, the negative in spectrum is usually represented the quantity of imaginary frequency.

After R_{nuclei}(t) in eq.(3.17) substituted into eq.(3.15), the integral with respect to t is perform from 0 to ∞[‡]. Therefore,

$$R(w) \sim \frac{[1 - e^{-\hbar\omega/k_BT}]}{\omega}\rho_{pol}(\omega). \tag{3.18}$$

This formula depicts the relation of $\rho_{pol}(\omega)$ and R(ω). $\left(1 - e^{-\hbar\omega/k_BT}\right)$ is the quantum correction factor. When $\hbar\omega \gg k_BT$, the factor $\left(1 - e^{-\hbar\omega/k_BT}\right)$ reduced to ω, and R(ω) can be represented by ρ_{pol}.

3.4 Collective polarizability of liquid water

3.4.1 Effective molecular polarizability

Consider the effective dipole moment $\boldsymbol{\mu}_i$ of molecule of liquid water in laser field $\boldsymbol{E}^{ext}$. Water molecule is a polar one, and has a permanent dipole moment $\boldsymbol{\mu}^p$. The extrinsic dipole moment of molecule i in liquid water is induced by laser field and polar molecules around it. Therefore, the effective dipole moment of molecule i in liquid water is

$$\boldsymbol{\mu}_i = \boldsymbol{\mu}_i^p + \boldsymbol{\alpha}_i^M \boldsymbol{E}^{ext} + \boldsymbol{\alpha}_i^M \sum_{j(\neq i)}^{N} \mathbf{T}_{ij} \cdot \boldsymbol{\mu}_j, \tag{3.19}$$

where $\mathbf{T}_{ij}$ is dipole interaction tensor given as $\mathbf{T}_{ij} = \frac{3\boldsymbol{r}_{ij}\boldsymbol{r}_{ij} - r_{ij}^2\boldsymbol{I}}{r_{ij}^5}$, and only depends on the distance between the center of mass of molecules i and j. $\mathbf{T}_{ij} \cdot \boldsymbol{\mu}_j$ is the electric field on molecule i due to molecule j.

The polarizability of molecule i in liquid water is defined as

$$\boldsymbol{\alpha}_i \equiv \lim_{E^{ext}\to 0} \frac{\partial \boldsymbol{\mu}_i}{\partial \boldsymbol{E}^{ext}}, \tag{3.20}$$

where $\boldsymbol{\mu}_i$ is given as eq.3.19. Thus

$$\begin{aligned} \boldsymbol{\alpha}_i &= \boldsymbol{\alpha}_i^M + \boldsymbol{\alpha}_i^M \sum_{j(\neq i)} \mathbf{T}_{ij} \frac{\partial \boldsymbol{\mu}_j}{\partial \boldsymbol{E}^{ext}} + \frac{\partial \boldsymbol{\alpha}_i^M}{\partial \boldsymbol{E}^{ext}} \sum_{j(\neq i)} \mathbf{T}_{ij}\boldsymbol{\mu}_j \\ &= \boldsymbol{\alpha}_i^M + \boldsymbol{\alpha}_i^M \sum_{j(\neq i)} \mathbf{T}_{ij}\boldsymbol{\alpha}_j + \boldsymbol{\beta}_i^M \sum_{j(\neq i)} \mathbf{T}_{ij}\boldsymbol{\mu}_j, \end{aligned} \tag{3.21}$$

where $\boldsymbol{\beta}_i^M \equiv \frac{\partial \boldsymbol{\alpha}_i^M}{\partial \boldsymbol{E}^{ext}}$ called the hyperpolarizability is the first derivative of $\boldsymbol{\alpha}_i^M$ with respect to electric field. The enhanced polarizability $\boldsymbol{\alpha}_j$ and dipole $\boldsymbol{\mu}_j$ are solved iteratively according to the two self-consistent equations, eq. 3.19 and eq. 3.21.

[‡] $\int_0^\infty \sin\omega t \sin\omega' t dt = \frac{\pi}{2}[\delta(\omega - \omega') - \delta(\omega + \omega')]$, and we do not care about the negative frequency.

3.4.2 Collective polarizability

Collective polarizability, denoted by $\mathbf{\Pi}$, can be expressed as superposition of the effective polarizability of molecules embedded in the condensed phase. The effective polarizability of every molecule is considered as point polarizability located at the center of mass.

$$\mathbf{\Pi} = \sum_i \boldsymbol{\alpha}_i \tag{3.22}$$

and from eq.(3.21)

$$\mathbf{\Pi} = \sum_i [\boldsymbol{\alpha}_i^M + \boldsymbol{\alpha}_i^M \cdot \sum_{j(\neq i)} \mathbf{T}_{ij} \cdot \boldsymbol{\alpha}_j + \boldsymbol{\beta}_i^M \cdot \sum_{j(\neq i)} \mathbf{T}_{ij} \cdot \boldsymbol{\mu}_j]. \tag{3.23}$$

$\mathbf{\Pi}$ can be separated to two parts, molecular polarizability and induced polarizability: $\mathbf{\Pi} = \mathbf{\Pi}^M + \mathbf{\Pi}^I$.

$$\mathbf{\Pi}^M = \sum_i \boldsymbol{\alpha}_i^M, \tag{3.24}$$

$$\mathbf{\Pi}^I = \sum_i (\boldsymbol{\alpha}_i^M \cdot \sum_{j(\neq i)} \mathbf{T}_{ij} \cdot \boldsymbol{\alpha}_j + \boldsymbol{\beta}_i^M \cdot \sum_{j(\neq i)} \mathbf{T}_{ij} \cdot \boldsymbol{\mu}_j). \tag{3.25}$$

The molecular part($\mathbf{\Pi}^M$) is the sum of isolated molecular polarizability. The induced part($\mathbf{\Pi}^I$) arises from the intermolecular interaction. In this thesis, only the first term of $\mathbf{\Pi}^I$, $\boldsymbol{\alpha}\mathbf{T}\boldsymbol{\alpha}$, which is the first order approximation of the enhanced polarizaility is considered. That is,

$$\mathbf{\Pi} = \sum_i [\boldsymbol{\alpha}_i^M + \boldsymbol{\alpha}_i^M \cdot \sum_{j(\neq i)} \mathbf{T}_{ij} \cdot \boldsymbol{\alpha}_j]. \tag{3.26}$$

This approximation regards $\boldsymbol{\alpha}_i^M$ as a constant with respect to $\boldsymbol{E}^{ext}$. Hence, the existence of dipole moment is excluded to collective polarizability. $\boldsymbol{\alpha}_j$ in eq.(3.26) is the solution of eq.(3.21), but here we take an approximation $\alpha_j \cong \alpha_j^M$. Therefore,

$$\mathbf{\Pi} = \sum_i [\boldsymbol{\alpha}_i^M + \boldsymbol{\alpha}_i^M \cdot \sum_{j(\neq i)} \mathbf{T}_{ij} \cdot \boldsymbol{\alpha}_j^M] \tag{3.27}$$

is used to calculate the weight of modes, $(\frac{\partial \Pi_{xz}}{\partial q_\alpha})^2$, in this thesis.

3.5 Decomposition of polarizability anisotropy INM spectrum $\rho_{pol}(\omega)$

To separate the translational and rotational parts in $\frac{\partial \Pi_{xz}}{\partial q_\alpha}$[19],

$$\frac{\partial \Pi_{xz}}{\partial q_\alpha} = \left(\frac{\partial \Pi_{xz}}{\partial q_\alpha}\right)^{trans} + \left(\frac{\partial \Pi_{xz}}{\partial q_\alpha}\right)^{rot}, \tag{3.28}$$

the projection operators are introduced as

$$\mathbf{P} = \mathbf{U}^T\mathbf{U} = \boldsymbol{\delta}, \tag{3.29}$$

whose elements

$$P_{\alpha\beta} = \sum_j \sum_\mu U_{\alpha,j\mu} U_{j\mu,\beta}. \tag{3.30}$$

Because $\mathbf{P}$ is just an identity matrix, we can write down the equality

$$\frac{\partial \Pi_{xz}}{\partial q_\alpha} = \sum_\beta P_{\alpha\beta} \frac{\partial \Pi_{xz}}{\partial q_\beta}. \tag{3.31}$$

By separating the project operator into the translational and rotational parts,

$$P_{\alpha\beta} = P^{trans}_{\alpha\beta} + P^{rot}_{\alpha\beta}, \tag{3.32}$$

we can obtain the translational and rotational portion of $\frac{\partial \Pi_{xz}}{\partial q_\alpha}$,

$$\begin{aligned} \left(\frac{\partial \Pi_{xz}}{\partial q_\alpha}\right)^{trans} &= \sum_\beta P^{trans}_{\alpha\beta} \frac{\partial \Pi_{xz}}{\partial q_\beta} \\ \left(\frac{\partial \Pi_{xz}}{\partial q_\alpha}\right)^{rot} &= \sum_\beta P^{rot}_{\alpha\beta} \frac{\partial \Pi_{xz}}{\partial q_\beta}, \end{aligned} \tag{3.33}$$

where

$$P^{trans}_{\alpha\beta} = \sum_j \sum_{\mu=1,2,3} U_{\alpha,j\mu} U_{j\mu,\beta} \text{ , and } P^{rot}_{\alpha\beta} = \sum_j \sum_{\mu=4,5,6} U_{\alpha,j\mu} U_{j\mu,\beta}. \tag{3.34}$$

According to derivative chain rule of differential,

$$\frac{\partial \Pi_{xz}}{\partial q_\alpha} = \sum_{k\mu} \frac{\partial \Pi_{xz}}{\partial z_{k\mu}} \frac{\partial z_{k\mu}}{\partial q_\alpha} = \sum_{k\mu} \frac{\partial \Pi_{xz}}{\partial z_{k\mu}} U_{k\mu,\alpha}, \tag{3.35}$$

to calculate the weight of each mode $\left(\frac{\partial \Pi_{xz}}{\partial q_\alpha}\right)^2$, $\frac{\partial \Pi_{xz}}{\partial z_{j\mu}}$ and the eigenvector are

needed. Derive eq.(3.27) with respect to $z_{k\mu}$,

$$\frac{\partial \mathbf{\Pi}}{\partial z_{k\mu}} = \underbrace{\sum_i \frac{\partial \boldsymbol{\alpha}_i^M}{\partial z_{k\mu}}}_{\left(\frac{\partial \mathbf{\Pi}^M}{\partial z_{k\mu}}\right)} + \underbrace{\sum_i \left(\frac{\partial \boldsymbol{\alpha}_i^M}{\partial z_{k\mu}} \sum_{j(\neq i)} \mathbf{T}_{ij} \boldsymbol{\alpha}_j^M + \boldsymbol{\alpha}_i^M \sum_{j(\neq i)} \mathbf{T}_{ij} \frac{\partial \boldsymbol{\alpha}_j^M}{\partial z_{k\mu}} \right)}_{\left(\frac{\partial \mathbf{\Pi}^I}{\partial z_{k\mu}}\right)^{rot}} +$$

$$\underbrace{\sum_i \left(\boldsymbol{\alpha}_i^M \sum_{j(\neq i)} \frac{\partial \mathbf{T}_{ij}}{\partial z_{k\mu}} \boldsymbol{\alpha}_j^M \right)}_{\left(\frac{\partial \mathbf{\Pi}^I}{\partial z_{k\mu}}\right)^{trans}}. \tag{3.36}$$

Hence, $\frac{\partial \Pi_{xz}}{\partial z_{j\mu}}$ includes three terms: the contribution due to isolated molecule, which are only associated with rotational motions, the translational and rotational parts due to DID interaction. The details of the calculations for these terms are given in Appendix B.

Now, there are two ways to decompose the polarizability anisotropy INM spectrum according to above analyses. One way is to decompose $\rho_{pol}(\omega)$ into the molecular, DID interaction and their cross components,

$$\begin{aligned} \rho_{pol}^{MM} &= \rho_{pol}^{MM}, \\ \rho_{pol}^{II} &= \rho_{pol}^{IrIr} + \rho_{pol}^{ItIt} + \rho_{pol}^{IrIt}, \\ \rho_{pol}^{MI} &= \rho_{pol}^{MIr} + \rho_{pol}^{MIt}. \end{aligned} \tag{3.37}$$

The other way is to decompose $\rho_{pol}(\omega)$ into the rotational and translational components and their cross terms,

$$\begin{aligned} \rho_{pol}^{Rot} &= \rho_{pol}^{MM} + \rho_{pol}^{MIr} + \rho_{pol}^{IrIr}, \\ \rho_{pol}^{Trans} &= \rho_{pol}^{ItIt}, \\ \rho_{pol}^{Cross} &= \rho_{pol}^{MIt} + \rho_{pol}^{IrIt}, \end{aligned} \tag{3.38}$$

where

$$\rho_{pol}^{MM} = \frac{15}{N\gamma^2}\left\langle \sum_{\alpha}\left(\frac{\partial \Pi_{xz}^{M}}{\partial q_\alpha}\right)^2 \delta(\omega-\omega_\alpha)\right\rangle, \tag{3.39a}$$

$$\rho_{pol}^{IrIr} = \frac{15}{N\gamma^2}\left\langle \sum_{\alpha}\left(\frac{\partial \Pi_{xz}^{I}}{\partial q_\alpha}\right)_{rot}^2 \delta(\omega-\omega_\alpha)\right\rangle, \tag{3.39b}$$

$$\rho_{pol}^{ItIt} = \frac{15}{N\gamma^2}\left\langle \sum_{\alpha}\left(\frac{\partial \Pi_{xz}^{I}}{\partial q_\alpha}\right)_{trans}^2 \delta(\omega-\omega_\alpha)\right\rangle, \tag{3.39c}$$

$$\rho_{pol}^{MIr} = \frac{30}{N\gamma^2}\left\langle \sum_{\alpha}\left(\frac{\partial \Pi_{xz}^{M}}{\partial q_\alpha}\right)\left(\frac{\partial \Pi_{xz}^{I}}{\partial q_\alpha}\right)_{rot} \delta(\omega-\omega_\alpha)\right\rangle, \tag{3.39d}$$

$$\rho_{pol}^{MIt} = \frac{30}{N\gamma^2}\left\langle \sum_{\alpha}\left(\frac{\partial \Pi_{xz}^{M}}{\partial q_\alpha}\right)\left(\frac{\partial \Pi_{xz}^{I}}{\partial q_\alpha}\right)_{trans} \delta(\omega-\omega_\alpha)\right\rangle, \tag{3.39e}$$

$$\textit{and } \rho_{pol}^{IrIt} = \frac{30}{N\gamma^2}\left\langle \sum_{\alpha}\left(\frac{\partial \Pi_{xz}^{I}}{\partial q_\alpha}\right)_{rot}\left(\frac{\partial \Pi_{xz}^{I}}{\partial q_\alpha}\right)_{trans} \delta(\omega-\omega_\alpha)\right\rangle. \tag{3.39f}$$

3.6 Voronoi polyhedral analyses of local structure effects on Raman spectrum

We apply Voronoi polyhedral analysis on depolarized Raman spectrum in order to investigate the local geometry and structure effect in liquid water. This is similar as the Voronoi analyses applied to the INM DOS of liquid water[2][6].

There are two ways of Voronoi polyhedra analyses applied to Raman spectrum in this research. One is to classify the collective polarizability into four groups and examine the variation of each sub-collective polarizability $\mathbf{\Pi}_L$ with normal coordinates; the other is to classify coordinates into four groups and to investigate the variation of collective polarizability with each group of coordinates. The former method is a classification before differential, while the later is a classification after differential. The details of the derived procedure are given in Appendix C.

To analysis the geometric effect of local structure of each molecules, the fraction of each group should be considered. Thus, the average contribution

per molecule in every group to the spectrum is given as

$$\rho_{pol}^{LL}(\omega) = \frac{15}{\gamma^2} \sum_{\alpha} \left\langle \frac{1}{N_L} \left(\frac{\partial \mathbf{\Pi}}{\partial q_\alpha} \right)_L^2 \delta(\omega - \omega_\alpha) \right\rangle ; \tag{3.40a}$$

$$\rho_{pol}^{LH}(\omega) = \frac{30}{\gamma^2} \sum_{\alpha} \left\langle \frac{1}{\sqrt{N_L N_H}} \left(\frac{\partial \mathbf{\Pi}}{\partial q_\alpha} \right)_L \left(\frac{\partial \mathbf{\Pi}}{\partial q_\alpha} \right)_H \delta(\omega - \omega_\alpha) \right\rangle , \tag{3.40b}$$

where eq.(3.40a) is the pure term due to group L and eq.(3.40b) is the cross term due to the group L and H. L and H can be I,II,III,or IV, but L$\neq$ H for eq.(3.40b) There are four pure terms and six cross terms. The detailed derivation is given in Appendix D.

Chapter 4

Results and Discussions

4.1 Polarizability anisotropy INM spectrum

The polarizability anisotropy INM spectra of liquid water are shown in Fig. 4.1. It is surprised to find that the results of decomposition by different ways (eq.(3.37) and eq.(3.38)) are extremely similar. The six components in eq.(3.39) are plotted in Fig. 4.2. It shows that $D_{pol}^{IrIr}(\omega)$, $D_{pol}^{MIr}(\omega)$ and $D_{pol}^{IrIt}(\omega)$ are small. This implies that the rotational part of DID interaction contributes insignificantly. If we neglect those extremely small terms, the dominant terms of the two ways of decomposition, eq.(3.37) and eq.(3.38), are the same. As only intrinsic molecular polarizability and $\boldsymbol{\alpha T \alpha}$ terms are considered, the rotational, translational, and rotational-translational cross contributions correspond to the intrinsic molecular(D_{pol}^{MM}), the interaction-induced(D_{pol}^{II}), and the rotational-translational cross (D_{pol}^{MI}) components, respectively.

4.2 Depolarized Raman spectrum

The polarizability anisotropy INM spectrum $\rho_{pol}(\omega)$ is related to depolarized Raman spectrum $R(\omega)$ that the experiment can directly measured. The factor $\left(\frac{1-e^{-\hbar\omega/k_BT}}{\omega}\right)$ in eq.(3.18) for our system (T=300K) amplifies the intensities at low frequencies. The interaction-induced component $R^{II}(\omega)$ and the low-frequency molecular component $R^{MM}(\omega)$ are enhanced due to the quantum correction from the classical dynamics. Thus, around 230 cm^{-1}, $R(\omega)$ is changed from a shoulder to a peak and around 800 cm^{-1}, $R(\omega)$ from a peak to a smooth shoulder.

Shown in Fig. 4.4, $R(\omega)$ is compared with the result of the time correlation function obtained by MD method[17]. Although the INM method is applied

for the short time dynamic, the shape of molecular part $R^{MM}(\omega)$ looks very similar for the two methods. However, there are differences in $R(\omega)$ between the results we obtain and that given in Ref.[17], in which not only $\boldsymbol{\alpha T \alpha}$ term, but also $\boldsymbol{\beta T \mu}$ and one step further in the level of approximation for induced collective polarizability are considered. The DID component, $R^{II}(\omega)$(or translational part $R^{trans}(\omega)$), in Fig. 4.3(a) contributes only in the region of low frequencies and almost vanishes beyond 500 cm^{-1}. This is the same with the translational part of DOS (Fig. 4.3(c)). However, as considering the higher-order approximation of $\mathbf{\Pi}^I$ Fig. 4.3(b), there is still contribution to $R(\omega)$ beyond 500 cm^{-1}. This means that the translational modes at high frequencies contribute more to Raman spectrum as the high-order terms of Π^I are considered.

The MI-cross term we calculated (Fig. 4.3(a)) is obviously much smaller than the other two components, but MI-cross component in Fig. 4.3(c) does not. The MI-cross term in Fig. 4.3(a) has a smaller hump at 150 cm^{-1} and becomes negative in high-frequency region; The differences mentioned above are attributed to approximation in $\mathbf{\Pi}^I$ we used and that of the INM method.

4.3 Voronoi polyhedral (VP) analyses of depolarized Raman spectrum

The results are shown in Fig. 4.5, 4.6, 4.7, and 4.8.

The pure terms due to the rotational part of depolarized Raman spectrum $R^{rot}_{LL}(\omega)$ are the same, no matter which method of the Voronoi analysis is used, because the formalism eq.(C.3) and (C.5) of them are the same. (Because the contribution from $R^{Irot}(\omega)$ is small, $R^{rot}(\omega)$ is dominated by $R^{MM}(\omega)$.) The main difference comes from $R^{trans}_{LH}(\omega)$. Each pure term $R^{trans}_{LL}(\omega)$ according to the coordinate classification has a peak at 60 cm^{-1} about, but the result according to the polarizaility classification does not. $R^{trans}_{LL}(\omega)$ of the two classifications have different formulism. Feynman diagrams are introduced to find out the difference of them.

The diagrams are given in Fig. 4.9. The derivation of translational interaction-induced part of $(\frac{\partial \mathbf{\Pi}}{\partial q_\alpha})$ in group L, $(\frac{\partial \mathbf{\Pi}}{\partial q_\alpha})^{I,trans}_L$, are shown in Fig. 4.10 with the polarizaility classification and Fig.4.11 with the coordinate classification. We easily find that the different terms and the same ones between the two methods by Feynman diagrams. In Fig. 4.12, two terms are the same in each

$(\frac{\partial \mathbf{\Pi}}{\partial q_\alpha})_L^{I,trans}$; while three terms are different. The weight of a mode in group L is a square of $(\frac{\partial \mathbf{\Pi}}{\partial q_\alpha})_L^{I,trans}$, so that there are 10 terms for $R_{LL}^{trans}(\omega)$, and 3 of them are the same; while there are 25 terms for $R_{LH}^{trans}(\omega)$, and 4 of them are the same.

The physical significances for liquid water are discussed in the following:

- Rotational part of $R(\omega)$

  For molecules with strongly aspherical VP, their local structures are basically tetrahedral[5] and the molecule is more ordered and hard to rotate. Therefore, as asphericity increase, the intensities at the high-frequency modes increase (Fig. 4.5(b) and 4.6(b)). This agrees with Ref.[6]. The results of classifying according to volume of VP are inverse to those of the asphericity , the larger the volume, the lower the frequency of modes (Fig. 4.7(b) and Fig. 4.8(b)). This means that the molecules with larger volume are easier to rotate.

- Translational part of $R(\omega)$

  There is no peak in $R_{LL}^{trans}(\omega)$ by polarizability classification; while there are by coordinate classification. It is worth to note that the total $R^{trans}(\omega)$ does not have peak around 60 cm^{-1}(Fig. 4.3), thus, this peak appearing in pure term $R_{LL}^{trans}(\omega)$ by coordinate classification may be attributed to the negative contribution of cross terms $R_{LH}^{trans}(\omega)$ to $R^{trans}(\omega)$. In Fig. 4.6(c), if we only consider pure terms, the larger the asphericity, the higher the intensity of spectrum. Thus, we recognize that the molecule with larger asphericity is tetrahedral. This imply that the peak is cage effect form by H-bond according to Santis et al.[4], who regard the higher intensity in DOS of liquid water than that of the nonhydragen liquid at the same frequency as the cage effect form by H-bonds. While in Fig. 4.8(c), $R_{LL}^{trans}(\omega)$ are ordered when neglecting $R_{L=1,L=1}^{trans}(\omega)$, the larger the volume, the higher the intensity of spectrum. This agrees with the interpretation of O...O...O bending[2].

Since Raman spectrum of VP group has cross terms, we can not obtain the direct information about the effect of the local structures like DOS as the VP analyses on Raman spectrum. Maybe we should try another classification methods beyond the two we adopted. For example, to obtain the weight of every mode for each group $\left(\frac{\partial \mathbf{\Pi}}{\partial q_\alpha}\right)_L^2$, classify first $\left(\frac{\partial \mathbf{\Pi}}{\partial q_\alpha}\right)$ by the method of

classifying coordinate and then perform multiplying total $\left(\frac{\partial \mathbf{\Pi}}{\partial q_\alpha}\right)$ to these four groups instead of squaring. This method is derive from the method of the VP applying to velocity autocorrelation function, as one classifies VP of the initial configuration. The detail derivation is in Appendix E.

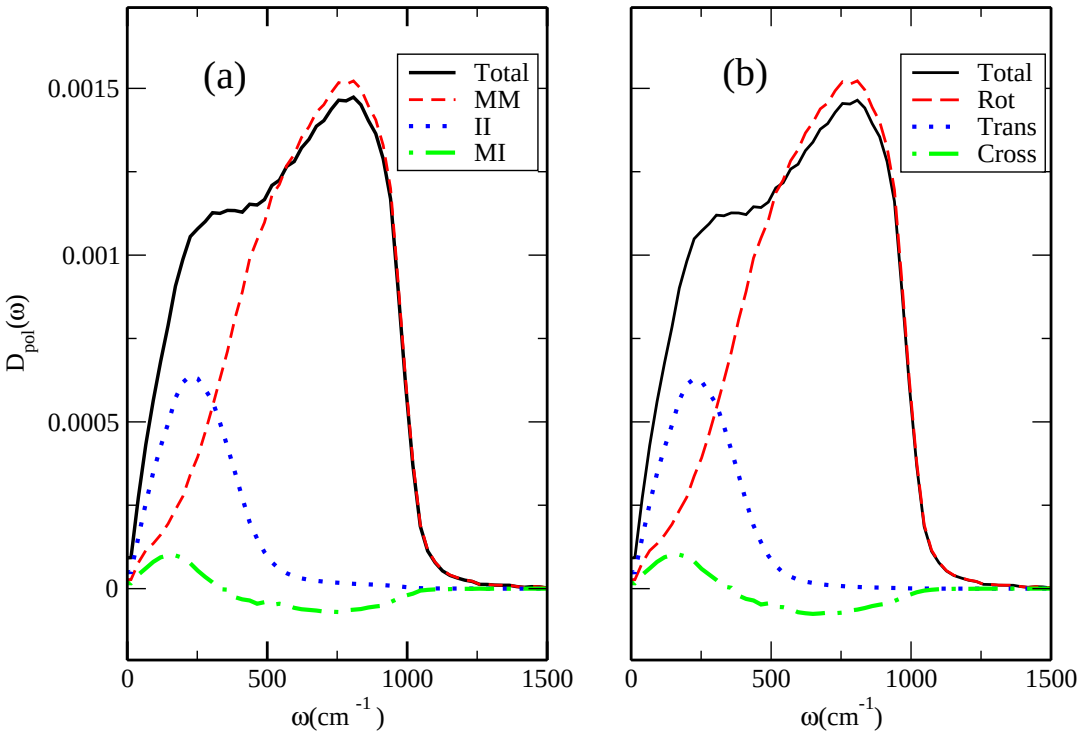

Figure 4.1: Normalized polarizability anisotropy INM spectrum $D_{pol}(\omega)$. (a) is the contributions of the molecule(MM), interaction-induced(II) and cross(MI) components; (b) is the rotational, translational and rotational-translational cross components.

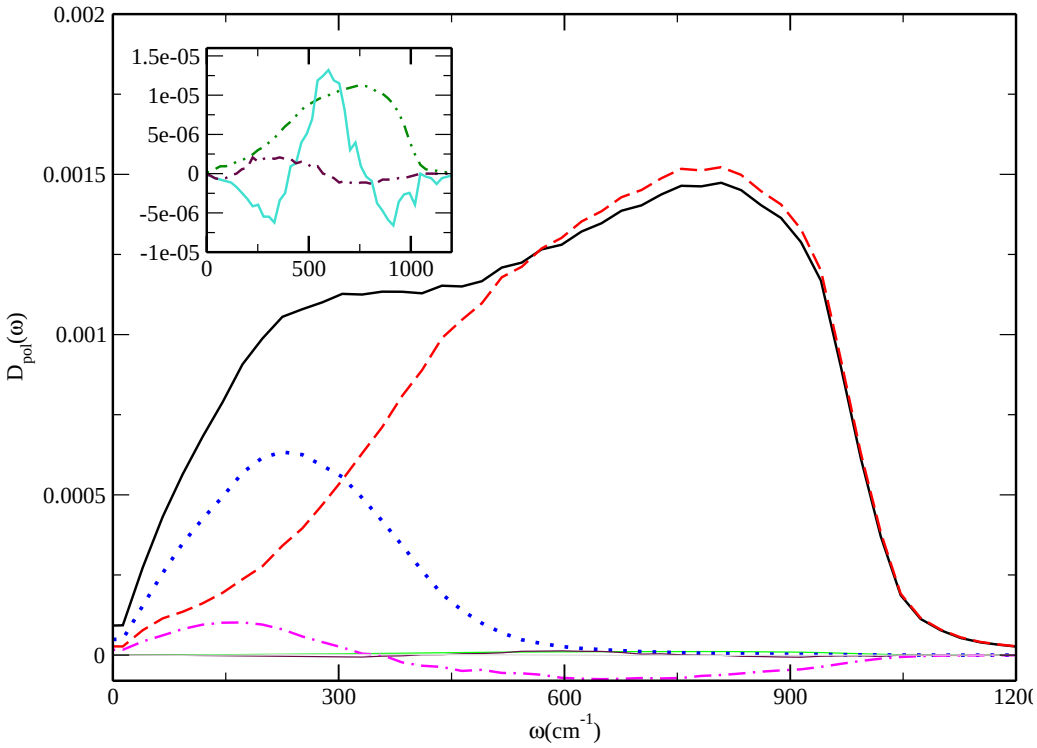

Figure 4.2: The six components of the normalized INM spectrum $D_{pol}(\omega)$: $D_{pol}^{Total}(\omega)$(solid line), D_{pol}^{MM}(dashed line), D_{pol}^{ItIt}(dotted line), and the D_{pol}^{MIt}(dot-dashed line). Inset shows terms whose contribution are small. The dot-dot-dashed line is $D_{pol}^{IrIr}(\omega)$, the dash-dash-dotted line is $D_{pol}^{MIr}(\omega)$, and the solid line is $D_{pol}^{IrIt}(\omega)$.

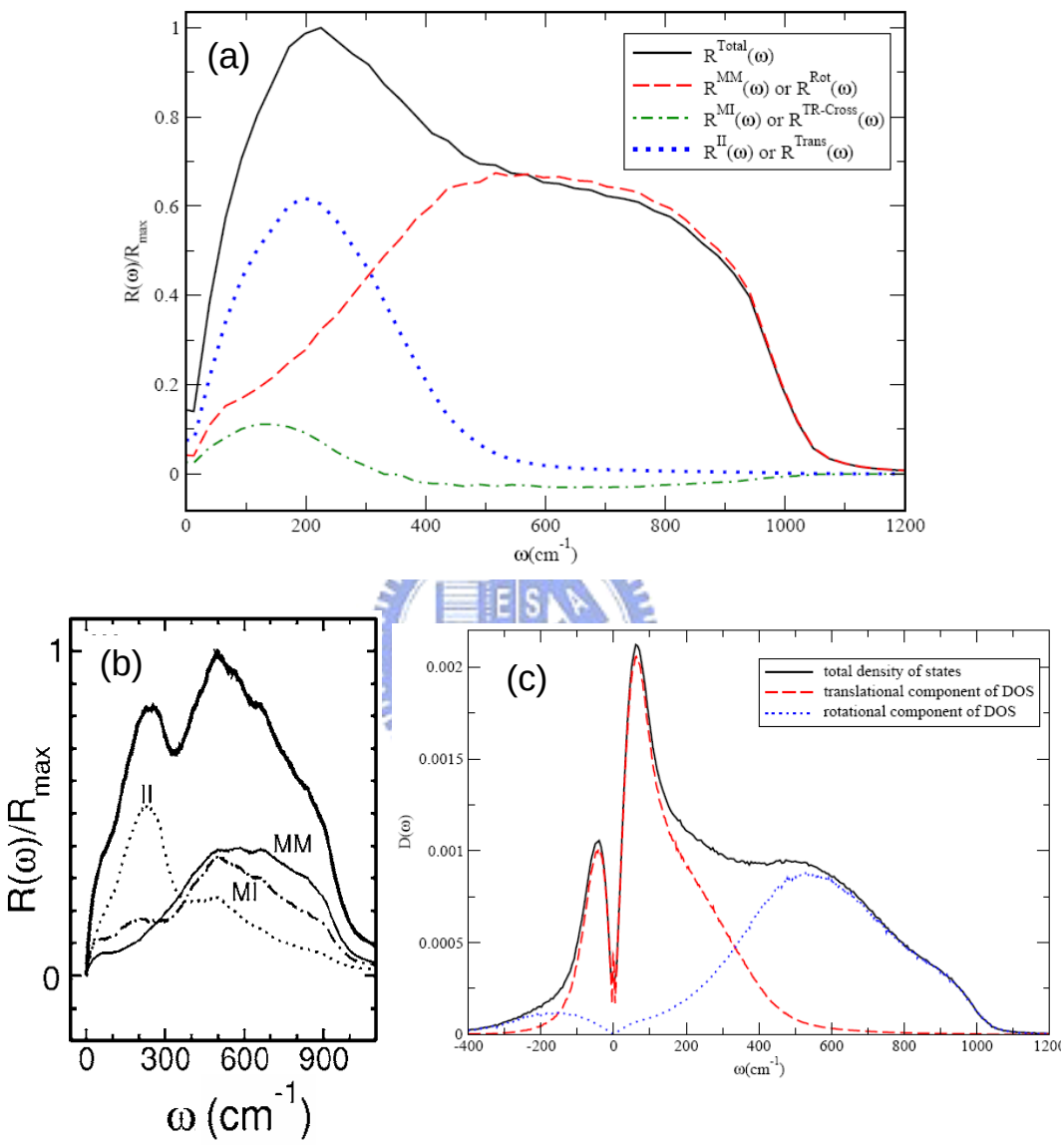

Figure 4.3: In (a), Depolarized Raman spectrum $R(\omega)$ calculated by the INM approach with only the intrinsic molecular polarizability and the $\boldsymbol{\alpha T \alpha}$ term being considered. (b) is the result $R(\omega)$ obtained by time correlation function[17]. In (c), the INM DOS of liquid water for SPC/E model [8].

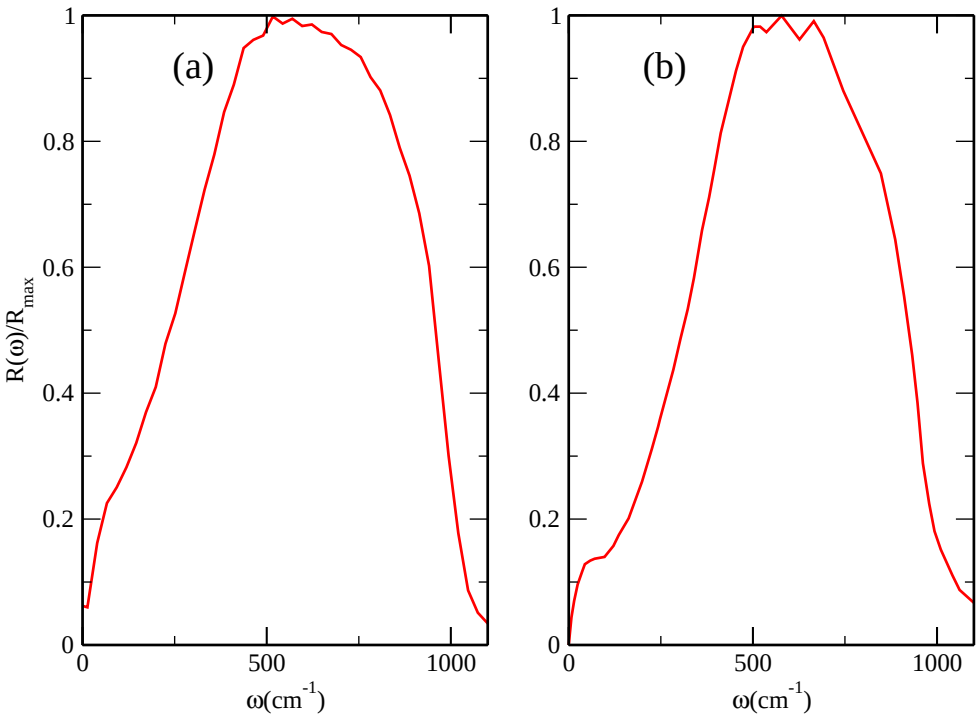

Figure 4.4: Depolarized Raman spectrum of MM component: (a)the INM approach, and (b)the MM line in Fig. 4.3(b).

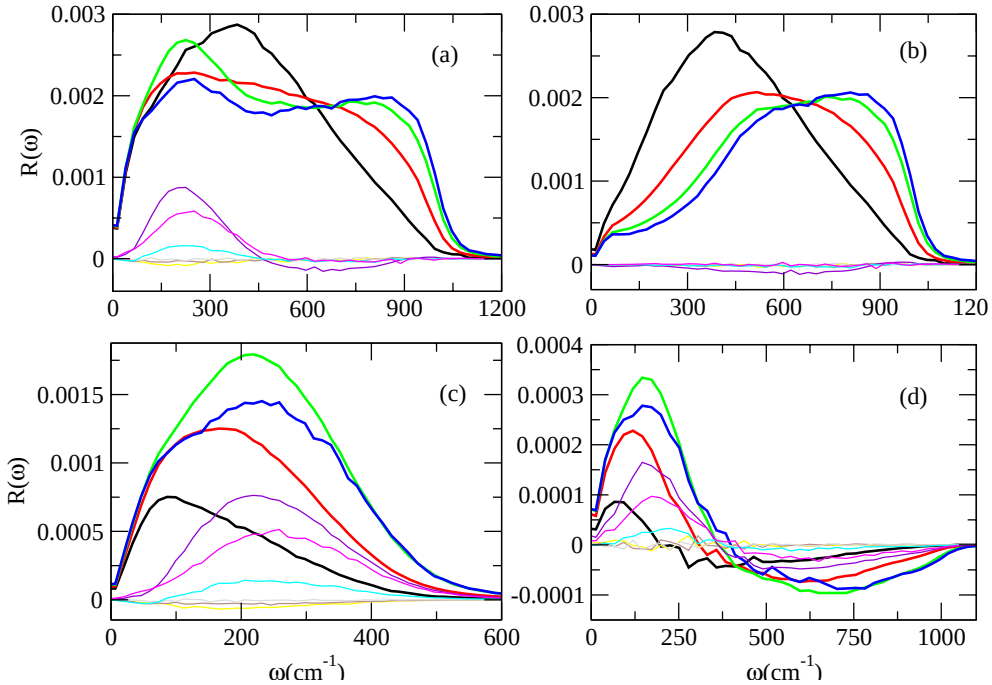

Figure 4.5: Voronoi analysis according to asphericity with polarizability classification. (a),(b),(c),(d) are $R_{LH}(\omega)$, $R^{rot}_{LH}(\omega)$(or $R^{MM}_{LH}(\omega)$), $R^{trans}_{LH}(\omega)$(or $R^{II}_{LH}(\omega)$), $R^{cross}_{LH}(\omega)$(or $R^{MI}_{LH}(\omega)$), respectively, where L, H=I, II, III, or IV group. Thick lines are the pure terms: black(11), red(22), green(33), blue(44). Thin lines are the cross terms: violet(23), magenta(34), etc. the symbol (LL) and (LH) is defined in eq. 3.40.

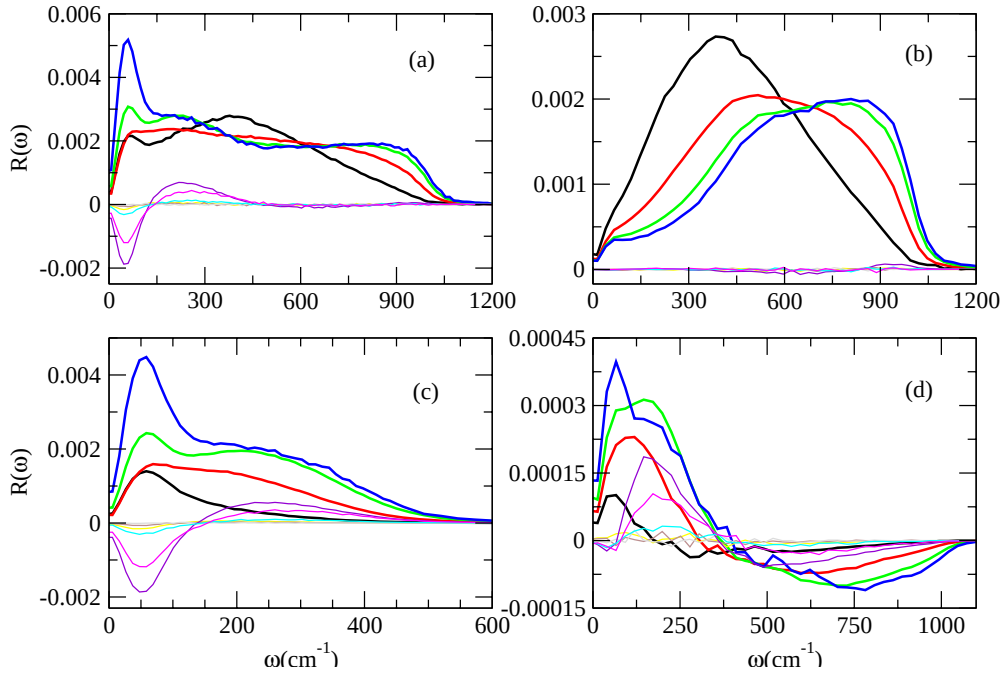

Figure 4.6: Voronoi analysis according to asphericity with the method of classifying coordinate. The order and the colors of lines are the same with Fig.4.5

.

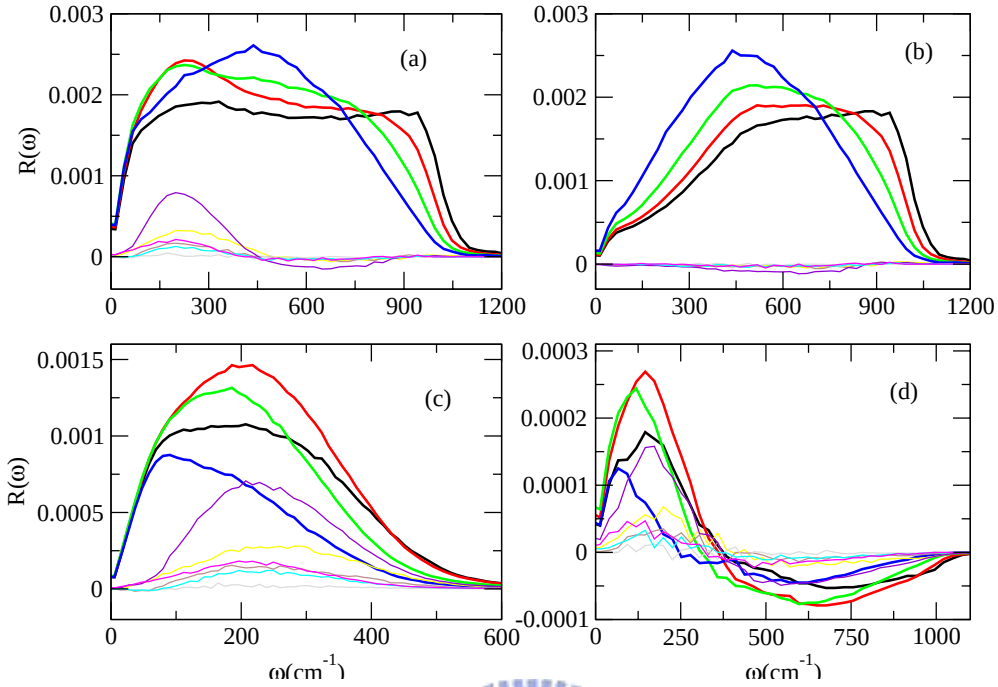

Figure 4.7: Voronoi analysis according to volume with the method of classifying polarizability. The order and colors of lines are the same with Fig.4.5.

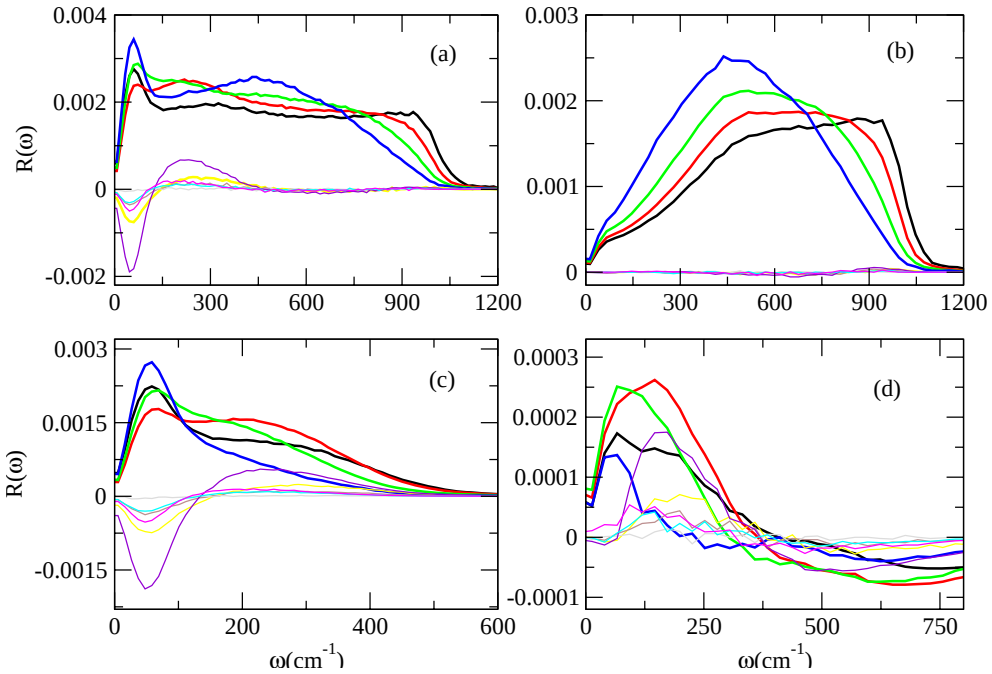

Figure 4.8: Voronoi analysis according to volume with the method of classifying coordinate. The order and the colors of lines are the same with Fig.4.5.

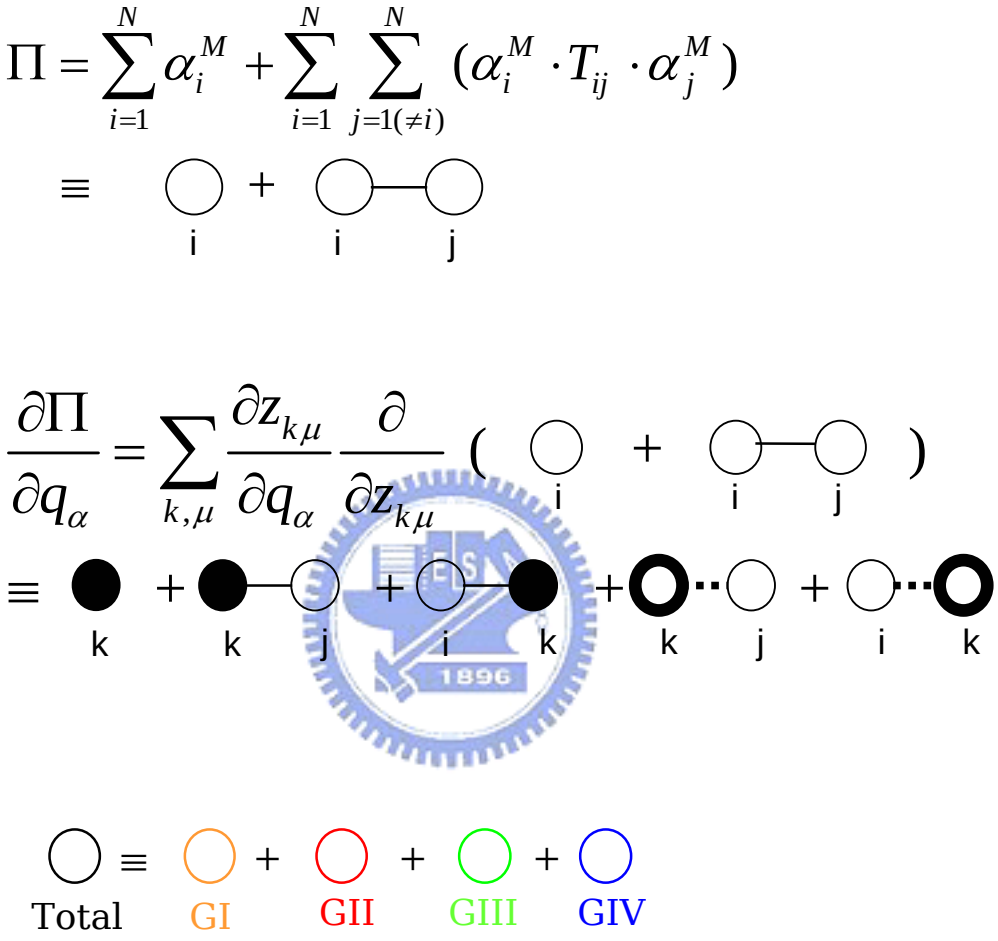

Figure 4.9: The diagrams representing collective polarizability and partial derivation with respect to the coordinate. Circles represent polarizability; thin solid lines represent dipole tensor $\boldsymbol{T}_{ij}$; disks represent differential polarizability; thick dotted lines represent $\frac{\partial \boldsymbol{T}_{ij}}{\partial z_k}$, and thick circles label k=i or k=j.

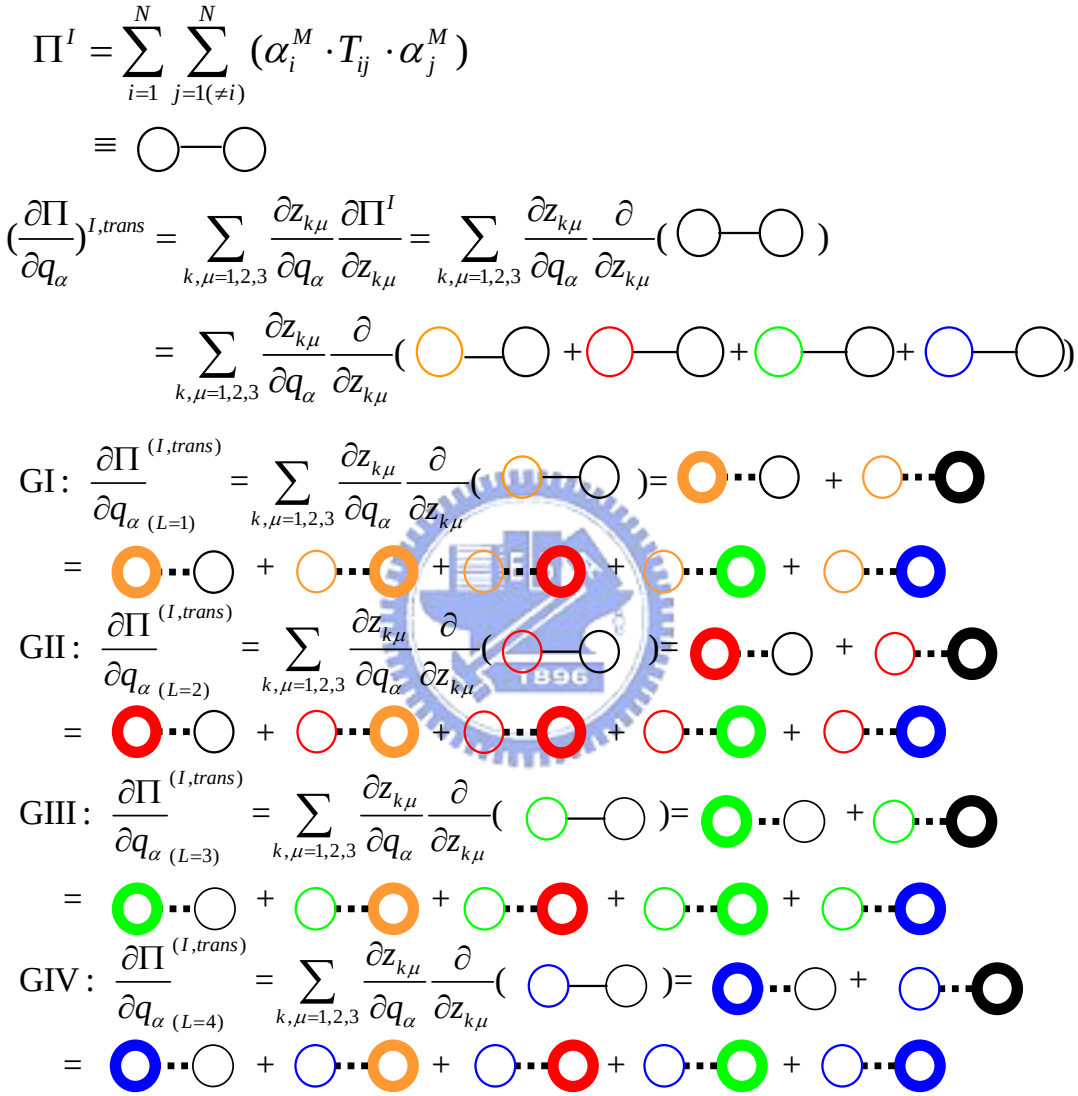

Figure 4.10: The derivation of translational induced-interaction part of $(\frac{\partial \mathbf{\Pi}}{\partial q_\alpha})$ in L group, $(\frac{\partial \mathbf{\Pi}}{\partial q_\alpha})^{I,trans}_{L}$ with polarizability classification.

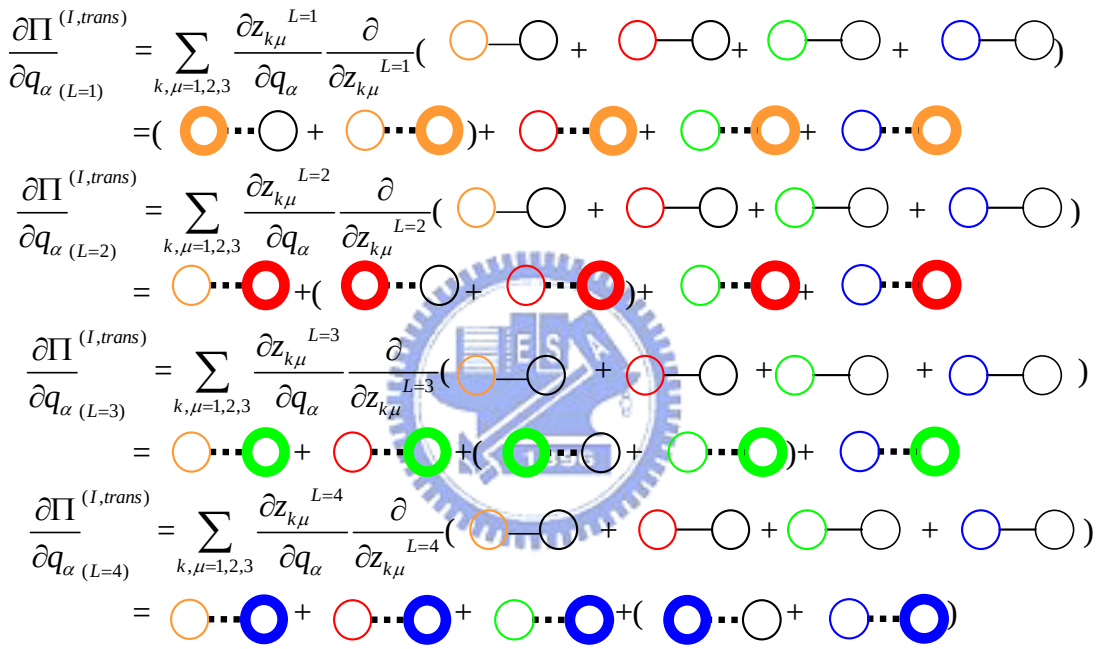

Figure 4.11: The derivation of translational induced-interaction part of $(\frac{\partial \mathbf{\Pi}}{\partial q_\alpha})$ in L group, $(\frac{\partial \mathbf{\Pi}}{\partial q_\alpha})_L^{I,trans}$ with coordinate classification.

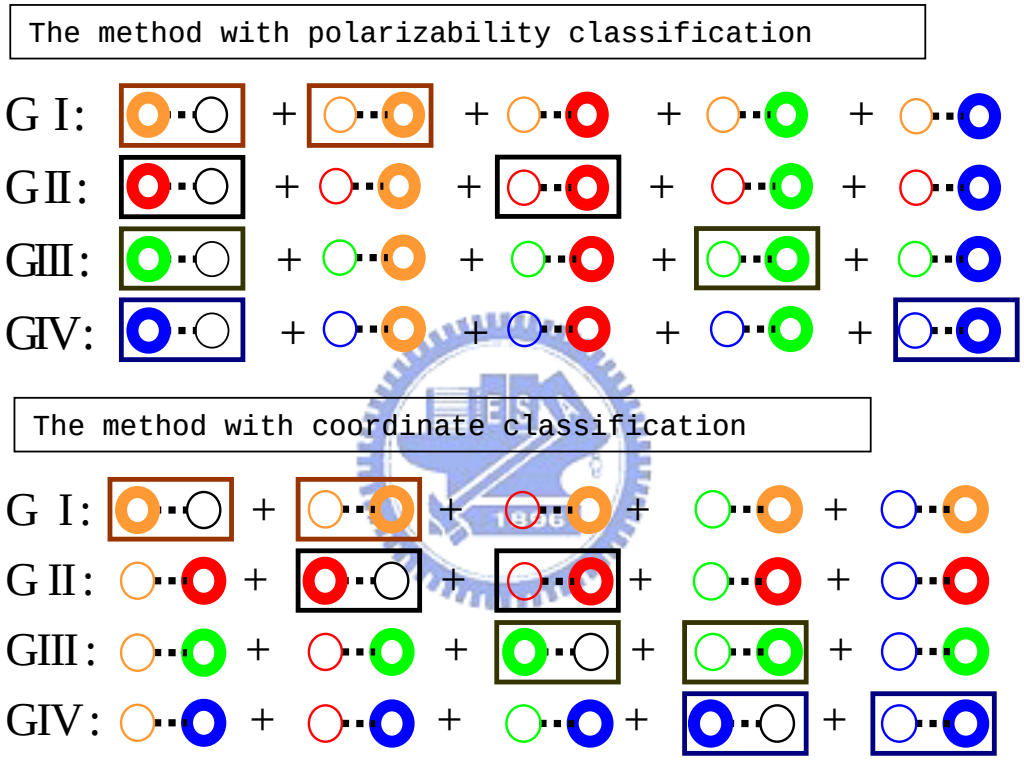

Figure 4.12: The 2 same terms and 3 different terms in $(\frac{\partial \mathbf{\Pi}}{\partial q_\alpha})_L^{I,trans}$ between polarizability classification and coordinate classification

Chapter 5

Conclusions

First, in this thesis, the method, different from MD method, based on INM theory is used to calculate Raman spectrum of liquid water. We identify the contributions of rotation, translation, and their cross correlations to polarizability anisotropy INM spectrum $\rho_{pol}(\omega)$, and another contributions: the molecular, DID interaction and their cross components. We find that the two ways of composition are the same as only considering $\boldsymbol{\alpha T \alpha}$ for $\mathbf{\Pi}^I$. We also find the 60 cm^{-1} peak in DOS vanish in the Raman spectrum.

Second, We compare $R(\omega)$ we calculate with that obtained from MD method and considered more accuracy for $\mathbf{\Pi}^I$. The molecular, DID interaction and their cross components are also compared. Although there is an approximation in INM method, but the MM component is similar to each other.

The last, the results with the classifications we used have cross terms and are not clear to identify the effect of local structures in Raman spectrum of liquid water. New application(VP analyses on Raman spectrum) is put into practice. Although there is no new discovery in the origin of the low frequency of liquid water, the VP analyses does succeed to separate Raman spectrum according to the parameters of VP.

Appendix A

List of notations

k_B: Bolzman constant
q: charge
m: mass of molecule
T: temperature
i, j, k: index of molecules
α, β: index of modes
N: the total number of molecules in the system
q_α:normal mode
η:asphericity of Voronoi cell
$\tilde{V}$:scaled volume of Voronoi cell
$\rho_{pol}(\omega)$: polarizability anisotropy INM spectrum
$\chi(\omega)$: OKE spectrum
$R(\omega)$: depolarized Raman spectrum
$R_{nuclei}(t)$: nuclear response function
$\Psi(t)$: time correlation function of the off-diagonal component of the collective polarizability tensor
γ: polarizability anisotropy
α^0: principle polarizability component
$G_{xz}(t)$: polarizability anisotropy velocity time correlation
$\boldsymbol{E}^{ext}$: external field
$\boldsymbol{\alpha}^M$: intrinsic molecular polarizability tensor
$\mathbf{\Pi}$: Collective polarizability tensor
$\mathbf{T}_{ij}$: dipole tensor between molecule i and j

Appendix B

Computational details of $\frac{\partial \Pi_{xz}}{\partial q_\alpha}$

The derivatives of the polarizability anisotropy with respect to mass-weighted coordinate, $\frac{\partial \Pi_{xz}}{\partial z_{k\mu}}$, include three terms:

- Isolated molecule contribution

$$\left(\frac{\partial \mathbf{\Pi}}{\partial z_{k\mu}}\right)^{M} = \sum_{i} \frac{\partial \boldsymbol{\alpha}_i^M}{\partial z_{k\mu}} = \frac{\partial \boldsymbol{\alpha}_k^M}{\partial z_{k\mu}} \tag{B.1}$$

- Rotational part of the dipole-induced-dipole contribution

$$\begin{aligned}\left(\frac{\partial \mathbf{\Pi}^I}{\partial z_{k\mu}}\right)^{rot} &= \sum_{i} \left(\frac{\partial \boldsymbol{\alpha}_i^M}{\partial z_{k\mu}} \sum_{j(\neq i)} \mathbf{T}_{ij} \boldsymbol{\alpha}_j^M + \boldsymbol{\alpha}_i^M \sum_{j(\neq i)} \mathbf{T}_{ij} \frac{\partial \boldsymbol{\alpha}_j^M}{\partial z_{k\mu}} \right) \\ &= \sum_{j=1}^{N} \frac{\partial \boldsymbol{\alpha}_k^M}{\partial z_{k\mu}} \mathbf{T}_{kj} \alpha_j^M + \sum_{i=1}^{N} \boldsymbol{\alpha}_i^M \mathbf{T}_{ik} \frac{\partial \boldsymbol{\alpha}_k^M}{\partial z_{k\mu}} \\ &= \sum_{p=1(\neq k)}^{N} \left(\frac{\partial \boldsymbol{\alpha}_k^M}{\partial z_{k\mu}} \mathbf{T}_{kp} \alpha_p + \boldsymbol{\alpha}_p^M \mathbf{T}_{pk} \frac{\partial \boldsymbol{\alpha}_k^M}{\partial z_{k\mu}} \right)\end{aligned} \tag{B.2}$$

- Translational part of the dipole-induced-dipole contribution

$$\begin{aligned}\left(\frac{\partial \mathbf{\Pi}^I}{\partial z_{k\mu}}\right)^{trans} &= \sum_{i} \left(\boldsymbol{\alpha}_i^M \sum_{j(\neq i)} \frac{\partial \mathbf{T}_{ij}}{\partial z_{k\mu}} \boldsymbol{\alpha}_j^M \right) \\ &= \sum_{j=1(\neq k)} \boldsymbol{\alpha}_k^M \frac{\partial \mathbf{T}_{kj}}{\partial z_{k\mu}} \boldsymbol{\alpha}_j^M + \sum_{i=1(\neq k)} \boldsymbol{\alpha}_i^M \frac{\partial \mathbf{T}_{ik}}{\partial z_{k\mu}} \boldsymbol{\alpha}_k^M \\ &= \sum_{p=1(\neq k)}^{N} \left(\boldsymbol{\alpha}_k^M \frac{\partial \mathbf{T}_{kp}}{\partial z_{k\mu}} \boldsymbol{\alpha}_p^M + \boldsymbol{\alpha}_p^M \frac{\partial \mathbf{T}_{pk}}{\partial z_{k\mu}} \boldsymbol{\alpha}_k^M \right)\end{aligned} \tag{B.3}$$

Because the system of liquid water is isotropic, off-diagonal elements of collective polarizability are the same. We average all off-diagonal elements of $\frac{\partial \mathbf{\Pi}}{\partial z_{k\mu}}$

as $\frac{\partial \Pi_{xz}}{\partial z_{k\mu}}$. Then, partial derivatives of Π_{xz} with respect to normal coordinates,

$$\left(\frac{\partial \Pi_{xz}}{\partial q_\alpha}\right)^{M} = \sum_{k} \sum_{\mu=4,5,6} \left(\frac{\partial \Pi_{xz}}{\partial z_{k\mu}}\right)^{M} U_{k\mu,\alpha} \tag{B.4a}$$

$$\left(\frac{\partial \Pi_{xz}}{\partial q_\alpha}\right)^{Irot} = \sum_{k} \sum_{\mu=4,5,6} \left(\frac{\partial \Pi_{xz}}{\partial z_{k\mu}}\right)^{Irot} U_{k\mu,\alpha} \tag{B.4b}$$

$$\left(\frac{\partial \Pi_{xz}}{\partial q_\alpha}\right)^{Itrans} = \sum_{k} \sum_{\mu=1,2,3} \left(\frac{\partial \Pi_{xz}}{\partial z_{k\mu}}\right)^{Itrans} U_{k\mu,\alpha} \tag{B.4c}$$

Appendix C

Computational details of Voronoi polyhedral analyses for Raman spectrum

The weight of mode α is $\left(\frac{\partial \mathbf{\Pi}}{\partial q_\alpha}\right)^2$. $\frac{\partial \mathbf{\Pi}}{\partial q_\alpha}$ can be classified to four groups,

$$\frac{\partial \mathbf{\Pi}}{\partial q_\alpha} = \sum_L \left(\frac{\partial \mathbf{\Pi}}{\partial q_\alpha}\right)_L . \tag{C.1}$$

In this thesis, there are two ways that we classify $\frac{\partial \mathbf{\Pi}}{\partial q_\alpha}$:

- Classification according to collective polarizabilities of subgroups

$$\because \quad \frac{\partial \mathbf{\Pi}}{\partial q_\alpha} = \frac{\partial \left[\mathbf{\Pi} \sum_L \Theta_i(L)\right]}{\partial q_\alpha} = \sum_L \underline{\left(\frac{\partial \left[\mathbf{\Pi}\Theta_i(L)\right]}{\partial q_\alpha}\right)} = \sum_L \underline{\left(\frac{\partial \mathbf{\Pi}}{\partial q_\alpha}\right)_L}, \tag{C.2}$$

$$\begin{aligned}
\therefore \left(\frac{\partial \mathbf{\Pi}}{\partial q_\alpha}\right)_L &= \frac{\partial \left[\mathbf{\Pi}\Theta_i(L)\right]}{\partial q_\alpha} = \sum_{k\mu} \frac{\partial z_{k\mu}}{\partial q_\alpha} \frac{\partial}{\partial z_{k\mu}} [\underbrace{\mathbf{\Pi}\Theta_i(L)}_{\mathbf{\Pi}_L}] \\
&= \sum_{k\mu} \frac{\partial z_{k\mu}}{\partial q_\alpha} \frac{\partial}{\partial z_{k\mu}} \sum_i [\boldsymbol{\alpha}_i \Theta_i(L) + \sum_i \boldsymbol{\alpha}_i \Theta_i(L) \sum_{j(\neq i)} \mathbf{T}_{ij} \boldsymbol{\alpha}_j] \\
&= \sum_{k\mu} \frac{\partial z_{k\mu}}{\partial q_\alpha} [\underbrace{\frac{\partial \boldsymbol{\alpha}_k}{\partial z_{k\mu}} \Theta_k(L)}_{\left(\frac{\partial \mathbf{\Pi}_L^M}{\partial z_{k\mu}}\right)} + \underbrace{\frac{\partial \boldsymbol{\alpha}_k}{\partial z_{k\mu}} \Theta_k(L) \sum_{j(\neq k)} \mathbf{T}_{kj} \boldsymbol{\alpha}_j + \sum_{i(\neq k)} \boldsymbol{\alpha}_i \Theta_i(L) \mathbf{T}_{ik} \frac{\partial \boldsymbol{\alpha}_k}{\partial z_{k\mu}}}_{\left(\frac{\partial \mathbf{\Pi}_L^I}{\partial z_{k\mu}}\right)^{rot}} + \\
&\underbrace{\boldsymbol{\alpha}_k \Theta_k(L) \sum_{j(\neq k)} \frac{\partial \mathbf{T}_{kj}}{\partial z_{k\mu}} \boldsymbol{\alpha}_j + \sum_{i(\neq k)} \boldsymbol{\alpha}_i \Theta_i(L) \frac{\partial \mathbf{T}_{ik}}{\partial z_{k\mu}} \boldsymbol{\alpha}_k}_{\left(\frac{\partial \mathbf{\Pi}_L^I}{\partial z_{k\mu}}\right)^{trans}}].
\end{aligned} \tag{C.3}$$

- Classification according to the coordinates of the subgroups

$$\because \quad \frac{\partial \mathbf{\Pi}}{\partial q_\alpha} = \frac{\partial \mathbf{\Pi}}{\partial q_\alpha} \sum_L \Theta_i(L) = \sum_L \underline{\left(\frac{\partial \mathbf{\Pi}}{\partial q_\alpha}\right) \Theta_i(L)} = \sum_L \underline{\left(\frac{\partial \mathbf{\Pi}}{\partial q_\alpha}\right)_L}, \tag{C.4}$$

$$\therefore \left(\frac{\partial \mathbf{\Pi}}{\partial q_\alpha}\right)_L = \left(\frac{\partial \mathbf{\Pi}}{\partial q_\alpha}\right) \Theta_i(L) = \sum_{k\mu} \frac{\partial z_{k\mu}}{\partial q_\alpha} \frac{\partial \mathbf{\Pi}}{\partial z_{k\mu}} \Theta_k(L) = \sum_{k\in L,\mu} \frac{\partial z^L_{k\mu}}{\partial q_\alpha} \frac{\partial \mathbf{\Pi}}{\partial z^L_{k\mu}}$$

$$= \sum_{k,\mu} \frac{\partial z_{k\mu}}{\partial q_\alpha} [\underbrace{\frac{\partial \boldsymbol{\alpha}_k}{\partial z_{k\mu}} \Theta_k(L)}_{\left(\frac{\partial \mathbf{\Pi}^M}{\partial z_{k\mu}}\right)_L} + \underbrace{\frac{\partial \boldsymbol{\alpha}_k}{\partial z_{k\mu}} \Theta_k(L) \sum_{j(\neq k)} \mathbf{T}_{kj} \boldsymbol{\alpha}_j + \sum_{i(\neq k)} \Theta_k(L) \boldsymbol{\alpha}_i \mathbf{T}_{ik} \frac{\partial \boldsymbol{\alpha}_k}{\partial z_{k\mu}}}_{\left(\frac{\partial \mathbf{\Pi}^I}{\partial z_{k\mu}}\right)^{rot}_L} +$$

$$\underbrace{\boldsymbol{\alpha}_k \Theta_k(L) \sum_{j(\neq k)} \frac{\partial \mathbf{T}_{kj}}{\partial z_{k\mu}} \boldsymbol{\alpha}_j + \sum_{i(\neq k)} \boldsymbol{\alpha}_i \frac{\partial \mathbf{T}_{ik}}{\partial z_{k\mu}} \Theta_k(L) \boldsymbol{\alpha}_k}_{\left(\frac{\partial \mathbf{\Pi}^I}{\partial z_{k\mu}}\right)^{trans}_L}]. \tag{C.5}$$

Appendix D

The derivation of the average contribution of spectrum per molecule in every group

Polarizability anisotropy INM spectrum

$$\begin{aligned}
\rho_{pol}(\omega) &= \frac{15}{\gamma^2 N}\sum_{\alpha}\left\langle\left(\frac{\partial\mathbf{\Pi}}{\partial q_\alpha}\right)^2\delta(\omega-\omega_\alpha)\right\rangle \\
&= \frac{15}{\gamma^2}\sum_{\alpha}\left\langle[\underbrace{\frac{1}{\sqrt{N}}\sum_{L}\left(\frac{\partial\mathbf{\Pi}}{\partial q_\alpha}\right)_L}_{eq.C.1}]^2\delta(\omega-\omega_\alpha)\right\rangle \\
&= \frac{15}{\gamma^2}\sum_{\alpha}\left\langle\left[\sum_{L}\sqrt{\chi_L}\frac{1}{\sqrt{N_L}}\left(\frac{\partial\mathbf{\Pi}}{\partial q_\alpha}\right)_L\right]^2\delta(\omega-\omega_\alpha)\right\rangle \\
&= \sum_{L}\rho'_{LL} + 2\sum_{L}\sum_{H(\neq L)}\rho'_{LH}, \qquad \text{(D.1)}
\end{aligned}$$

where

$$\rho'_{LL} = \frac{15}{\gamma^2}\chi_L\frac{1}{N_L}\sum_{\alpha}\left\langle\left(\frac{\partial\mathbf{\Pi}}{\partial q_\alpha}\right)^2_L\delta(\omega-\omega_\alpha)\right\rangle \qquad \text{(D.2)}$$

$$\rho'_{LH} = \frac{15}{\gamma^2}\sqrt{\chi_L\chi_H}\frac{1}{\sqrt{N_L N_H}}\sum_{\alpha}\left\langle\left(\frac{\partial\mathbf{\Pi}}{\partial q_\alpha}\right)^2_L\delta(\omega-\omega_\alpha)\right\rangle \qquad \text{(D.3)}$$

χ_L is average fraction of L over configurations, $\chi_L = \frac{N_L}{N}$. N_L is average number of molecules in L group. Thus, the average contribution of spectrum

per molecule in every group

$$\rho_{LL} = \frac{15}{\gamma^2}\frac{1}{N_L}\sum_{\alpha}\left\langle\left(\frac{\partial\mathbf{\Pi}}{\partial q_\alpha}\right)_L^2\delta(\omega-\omega_\alpha)\right\rangle \tag{D.4}$$

$$\rho_{LH} = \frac{15}{\gamma^2}\frac{1}{\sqrt{N_L N_H}}\sum_{\alpha}\left\langle\left(\frac{\partial\mathbf{\Pi}}{\partial q_\alpha}\right)_L^2\delta(\omega-\omega_\alpha)\right\rangle \tag{D.5}$$

Appendix E

The derivation of another kind of method beyond we used for example

From eq.(3.10), polarizability anisotropy velocity time correlation

$$G_{xz}(t) \cong \frac{15}{N\gamma^2}\langle\sum_{\alpha}(\frac{\partial\Pi_{xz}}{\partial q_\alpha})_{t=0}\dot{q}_\alpha(0)\sum_{\beta}(\frac{\partial\Pi_{xz}}{\partial q_\beta})_{t=0}\dot{q}_\beta(t)\rangle.$$

According to the method of the VP analysis applying to velocity autocorrelation function, only initial configurations are performed classifying. Thus,

$$\begin{aligned}
G_{xz}(t) &\cong \frac{15}{N\gamma^2}\langle\sum_{\alpha}(\frac{\partial\Pi_{xz}}{\partial q_\alpha})_{t=0}\dot{q}_\alpha(0)\sum_{L}\Theta_i(L)\sum_{\beta}(\frac{\partial\Pi_{xz}}{\partial q_\beta})_{t=0}\dot{q}_\beta(t)\rangle \\
&= \frac{15}{N\gamma^2}\langle\sum_{\alpha}<[(\frac{\partial\Pi_{xz}}{\partial q_\alpha})\sum_{L}\Theta_i(L)](\frac{\partial\Pi_{xz}}{\partial q_\alpha})>\underbrace{<\dot{q}_\alpha(0)\dot{q}_\beta(t)>}_{k_BT\cos\omega_\alpha t} \\
&= \frac{15}{N\gamma^2}\langle\sum_{\alpha}<[(\frac{\partial\Pi_{xz}}{\partial q_\alpha})\sum_{L}\Theta_i(L)](\frac{\partial\Pi_{xz}}{\partial q_\alpha})>k_BT\cos\omega_\alpha t \\
&= k_BT\int\rho_{pol}(\omega)\cos\omega t d\omega
\end{aligned} \tag{E.1}$$

Thus,

$$\rho_{pol} = \frac{15}{N\gamma^2}\sum_{\alpha}\langle\left[\frac{\partial\Pi_{xz}}{\partial q_\alpha}\sum_{L}\Theta_k(L)\right]\frac{\partial\Pi_{xz}}{\partial q_\alpha}\delta(\omega-\omega_\alpha)\rangle, \tag{E.2}$$

where $\left[\frac{\partial\Pi_{xz}}{\partial q_\alpha}\sum_{L}\Theta_k(L)\right]$ is classification according to coordinates of the subgroups in Appendix C.

Bibliography

[1] J. À Padró, J. Marti, J. Chem, Phys. 118, 452 (2003).

[2] K. H. Tsai and T. M. Wu, Chem. Phys. Lett. 417, 390 (2005).

[3] G. E. Walrafen, Y. C. Chu, and G. J. Piermarini, J. Chem, Phys. 100, 10363 (1996).

[4] A. D. Santis, A. Ercoli, D.Rocca, J. Chem Phys. 120, 1657 (2004).

[5] Y.L. Yeh and C. Y. Mou, J. Phys. Chem. B 103, 3699 (1999).

[6] S. L. Chang and T. M. Wu, and C. Y. Mou, J. Chem. Phys. 121, 3605 (2004).

[7] J.Szudy, Spectral Line Shapes, p649 (1989).

[8] S. L. Chang, Short-time dynamics of simple liquids and water/ the instantaneous normal mode analysis, PhD thesis.

[9] http://www.lsbu.ac.uk/water/models

[10] Stephen T. Thornton, Jerry B. Marion, classical dynamics of particles and systems Ch.12 (5th edt.)

[11] M. Cho, G. R. Fleming, S. Satio, I. Ohmine, and R. M. Stratt, J. Chem, Phys. 100, 6672 (1994).

[12] M. Buchner, B. M. Ladanyi, and R. M. Stratt, J. Chem, Phys. 97, 8522 (1992).

[13] K. Huang, Statistical Mechanics, Ch.6 (1987).

[14] H. Goldstein, Classical Mechanics, 3ed (2002).

[15] L. D. Landau and E.M.Lifshitz, Mechanics. §35 (3rd edt.)

[16] H. Torii, Chem. Phys. Lett. 353, 431 (2002).

[17] M. Dolores Elola and Branka M. Ladanyi, J. Chem. Phys. 126, 84504 (2007).

[18] J. P. Hansen and I. R. McDonald, Theory of simple liquid, Ch.7 (1976).

[19] Branka M. Ladanyi and Shannon Klein, J. Chem. Phys. 105,1552 (1996).

[20] M. S. Skafa and S. M. Vechi, J. Chem. Phys. 119, 2181 (2003).

Table 1: The parameters of SPC/E model: charges, angle between OH bond, OH bond length, LJ potential parameters in eq. 2.1 [9]

q_H(e)	q_O (e)	$\theta(^o)$	l($\mathring{A}$)	$\sigma(\mathring{A})$	ε(kJ mol^{-1})
+0.4238	-0.8476	109.47	1	3.166	0.650

Table 2: elements of polarizability tensor in body frame, and the coordinate is Fig. 2.3 [20]

α_{xx}	α_{yy}	α_{zz}
1.17	1.04	1.00

Table 3: Definition of Voronoi polyhedral groups according to asphericity and Voronoi volume V scaled by the averaged molecular volume, V_{avg} ($\tilde{\text{V}}$=$\frac{V}{V_{avg}}$) [2][6]

Group I	Group II	Group III	Group IV
$\eta \leq 1.46$	$1.46 < \eta \leq 1.72$	$1.72 < \eta \leq 1.98$	$1.98 < \eta$
$\tilde{V} \leq 0.84$	$0.84 < \tilde{V} \leq 1.0$	$1.0 < \tilde{V} \leq 1.24$	$1.24 < \tilde{V}$